Geochemistry, Geophysics, Geosystems

RESEARCH ARTICLE
10.1029/2018GC007739

Key Points:
- Paleomagnetic data from central Baja California yield a paleolatitudinal plate motion history equal to that of North America since Late Triassic time
- Seismic tomographic images demonstrate continuous long-lived eastward subduction of eastern Panthalassa lithosphere below Mexico
- Alternating phases of upper plate extension and shortening are correlated to flat and steep segments of the imaged slab

Supporting Information:
- Supporting Information S1
- Data Set S1
- Data Set S2
- Movie S1

Correspondence to:
L. M. Boschman,
lydianboschman@gmail.com

Citation:
Boschman, L. M., van Hinsbergen, D. J. J., Kimbrough, D. L., Langereis, C. G., & Spakman, W. (2018). The dynamic history of 220 Million Years of subduction below Mexico: A correlation between slab geometry and overriding plate deformation based on geology, paleomagnetism, and seismic tomography. *Geochemistry, Geophysics, Geosystems*, *19*, 4649–4672. https://doi.org/10.1029/2018GC007739

Received 7 JUN 2018
Accepted 26 NOV 2018
Accepted article online 28 NOV 2018
Published online 20 DEC 2018

The Dynamic History of 220 Million Years of Subduction Below Mexico: A Correlation Between Slab Geometry and Overriding Plate Deformation Based on Geology, Paleomagnetism, and Seismic Tomography

Lydian M. Boschman[1], Douwe J. J. van Hinsbergen[1], David L. Kimbrough[2], Cor G. Langereis[1], and Wim Spakman[1,3]

[1]Department of Earth Sciences, Utrecht University, Utrecht, Netherlands, [2]Department of Geological Sciences, San Diego State University, San Diego, CA, USA, [3]Center for Earth Evolution and Dynamics, University of Oslo, Oslo, Norway

Abstract Global tectonic reconstructions of pre-Cenozoic plate motions rely primarily on paleomagnetic and geological data from the continents, and uncertainties increase significantly with deepening geological time. In attempting to improve such deep-time plate kinematic reconstructions, restoring lost oceanic plates through the use of geological and seismic tomographical evidence for past subduction is key. The North American Cordillera holds a record of subduction of oceanic plates that composed the northeastern Panthalassa Ocean, the large oceanic realm surrounding Pangea in Mesozoic times. Here we present new paleomagnetic data from subduction-related rock assemblages of the Vizcaíno Peninsula of Baja California, Mexico, which yield a paleolatitudinal plate motion history equal to that of the North American continent since Late Triassic time. This indicates that the basement rocks of the Vizcaíno Peninsula formed in the forearc of the North American Plate, adjacent to long-lived eastward dipping subduction at the southern part of the western North American continental margin. Tomographic images confirm long-lived, uninterrupted eastward subduction. We correlate episodes of overriding plate shortening and extension to flat and steep segments of the imaged slab. By integrating paleomagnetic, geological, and tomographic evidence, we provide a first-order model that reconciles absolute North American plate motion and the deformation history of Mexico since Late Triassic time with modern slab structure.

Plain Language Summary Reconstruction of deep-time global tectonic plate motions relies primarily on data derived from the rock record of the continents, as the vast majority of pre-Cenozoic oceanic crust has been recycled into the Earth's mantle in subduction zones. To improve deep-time plate tectonic reconstructions, adding information on the plate motions and the geometry of lost oceanic plates is therefore key. In this study, we attempt at reconstructing the subduction of oceanic plates of the eastern Panthalassa Ocean, which surrounded the supercontinent Pangea. We present new paleomagnetic data from the geological record of the Vizcaíno Peninsula of central Baja California and conclude that the Vizcaíno peninsula has since ~220 Ma been part of the North American Plate below which the Panthalassa plates subducted. Furthermore, we analyze mantle tomographic images, illustrating the presence of an extraordinary long anomaly interpreted as subducted lithosphere. By integrating geological, paleomagnetic, and seismic tomographic data, we present a model that reconciles absolute North American plate motion and the deformation history of Mexico since the Triassic with modern slab structure.

1. Introduction

Global tectonic reconstructions of pre-Cenozoic plate motions rely primarily on paleomagnetic and geological data from the continents, as the vast majority of Mesozoic and older oceanic lithosphere has been lost to subduction. As a result, deep-time reconstructions portray the distribution of continental plates through geological time but lack information on plate motions and geometry in the oceanic domains. In attempting to improve such deep-time plate kinematic reconstructions, restoring lost oceanic plates is therefore key. This relies on deciphering the geological history of relics of such plates now found within orogenic belts or accretionary prisms (e.g., Domeier et al., 2017; Gürer et al., 2016; Maffione et al., 2017; Nokleberg, 2000). In parallel, the analysis of seismic tomography models of present-day mantle structure contributes to the development of paleogeographic models and tectonic reconstructions. (e.g., Domeier et al., 2017; Sigloch & Mihalynuk,

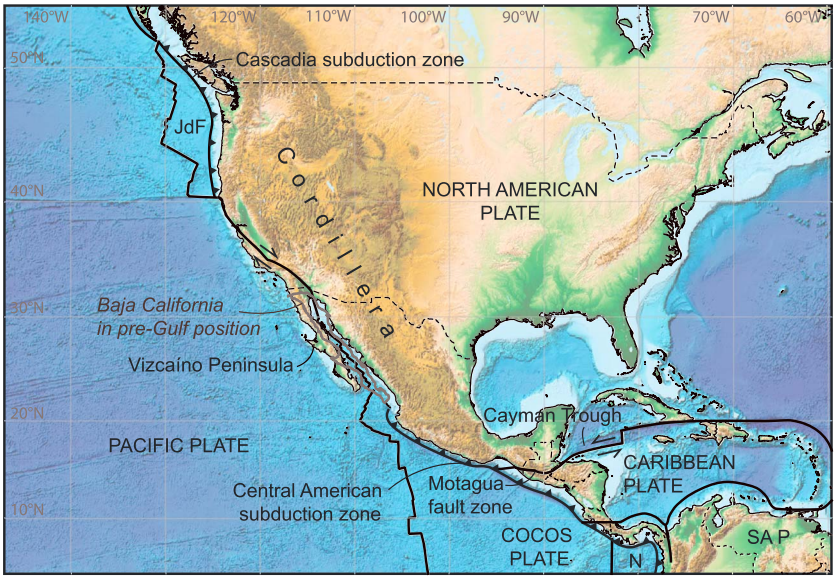

Figure 1. Tectonic map of the North American Cordillera, including the North American, South American (SA P), Caribbean, Pacific, Juan de Fuca (JdF), Cocos and Nazca (N) plates. Also including the position of Baja California prior to Gulf of California opening relative to a stable North American Plate.

2013; van der Meer et al., 2012; Van der Voo et al., 1999a, 1999b; Wu et al., 2016). Correlations of preserved geological subduction records to imaged mantle structure suggest that the mantle holds a memory of ~250–300 Myr of subduction (Butterworth et al., 2014; Hafkenscheid et al., 2006; van der Meer et al., 2010, 2018; Van der Voo et al., 1999a; van Hinsbergen et al., 2005). Here we present a combined analysis focused on the subduction history below Mexico by using a combination of geological and paleomagnetic data and tomographic evidence for deep mantle subduction.

The North American Cordillera comprises the intensely deformed western part of the North American continent and preserves a geological record of subduction of oceanic plates that were once underlying the northeastern paleo-Pacific or Panthalassa Ocean, such as the Farallon and Kula plates (Debiche et al., 1987; Engebretson et al., 1985). This record of subduction resulted from both overriding plate deformation (i.e., the opening and closure of fore-and backarc basins and formation of overriding plate and Andean-style fold-thrust belts), as well as the accretion of far-traveled intraoceanic arcs, oceanic plateaus, deep marine sediments, and ophiolites (e.g., Nokleberg, 2000). In line with the geological evidence of a complex, long-lived history of subduction, a mosaic of positive wave speed anomalies interpreted as (mainly detached) subducted slab remnants are present below North America and the present-day Pacific realm (e.g., Liu et al., 2010; Sigloch & Mihalynuk, 2013; van der Meer et al., 2012, 2018). Linking such detached slabs to surface records of subduction requires control on absolute plate motions (i.e., plate motion relative to the lower mantle) and is challenging. The best constrained absolute plate motion frames, based on hot spots (Doubrovine et al., 2012; O'Neill et al., 2005), do not extend further back in time than ~120–130 Ma. Reference frames for earlier times are based on paleomagnetism (with or without true polar wander correction) and have therefore no absolute paleolongitudinal control (Steinberger & Torsvik, 2008; Torsvik et al., 2012). Recent frames have attempted to provide such control using correlation of surface geology to deep mantle structure (Torsvik & Cocks, 2016; van der Meer et al., 2010) but remain subject to large uncertainties. As a consequence, correlations of seismic tomography to Mesozoic Cordilleran subduction records have led to paleogeographic interpretations that are markedly different for pre-mid-Cretaceous times, which are best summarized by scenarios with (Shephard et al., 2013; van der Meer et al., 2012) or without (Sigloch & Mihalynuk, 2013, 2017) subduction directly under the North American continental margin.

Contrary to ancient subduction and detached slabs, the establishment of a link between a mantle anomaly and a geological subduction record is straightforward for active subduction. Today, the Juan de Fuca and Cocos plates, both considered relics of the Farallon Plate, subduct eastward below the continental margin

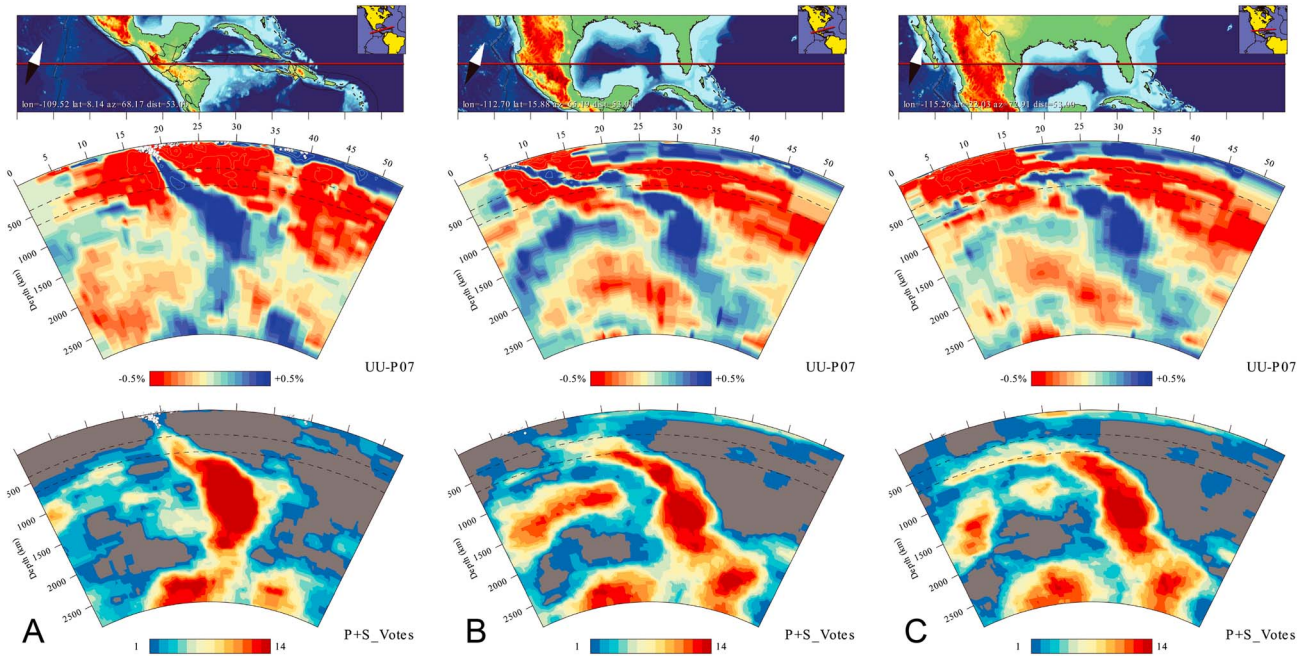

Figure 2. Seismic tomographic cross sections along great circle segments (straight horizontal line in geographic maps) of the Cocos slab (central panels). (a) Section south of the North American-Caribbean plate boundary. (b) North of this boundary. (c) Across southern Baja California. The tomographic model is the *P* wave seismic velocity model UU-P07 (Amaru, 2007). Units along the great circle arc are degrees measured from the start of the section. The lower panels show votemaps of seven seismic *P* wave velocity and seven *S* wave velocity models (Shephard et al., 2017).

of North America (Figure 1). Seismic tomography shows that subduction of the Juan de Fuca Plate at the Cascadia subduction zone is associated with a short upper mantle slab that is thought to represent only the last 16–18 Myr of subduction (Obrebski et al., 2010; van der Meer et al., 2018). On the contrary, the slab connected to the Cocos Plate, subducting below Mexico and Central America, is the longest apparently continuous slab, stretching from the uppermost mantle at the Central American trench in the west toward the lowermost mantle below the Atlantic Ocean in the east (Figure 2). This slab represents the lithosphere that was consumed at a long-lived plate boundary between the Panthalassa plate system and the Indo-Atlantic plate system, thereby providing a measure for relative plate motions between the two, as well as a starting point for the interpretation of the much more complex mantle structure surrounding this slab, related to subduction below and west of the Americas and the Caribbean region.

In Mexico, subduction-related rock assemblages are present that date back to the Triassic. Boschman et al. (2018) recently showed that Lower Cretaceous and younger records of subduction in Mexico tracked the paleolatitudinal motion of North America and may thus be readily tied to the (deforming) North American Plate. Older records associated with subduction are exposed in the Vizcaíno-Cedros region of Baja California, but it remains unknown whether these represent far-traveled intraoceanic subduction relics that were accreted to the North American margin or whether these also were part of the deforming North American upper plate. If the former, they provide no constraints on the age of subduction initiation below the Mexican continental margin, if the latter, they would show sustained subduction since the Triassic. Either way, the record may provide key constraints on the longevity of continental margin subduction below Mexico.

Here we present new paleomagnetic data from Triassic suprasubduction zone (SSZ) ophiolitic, as well as Jurassic arc-related sedimentary cover rocks from the Vizcaíno Peninsula of west central Baja California, and compile previous results, to test whether these rock units may be considered part of the (deforming) North American upper plate. We use the results to evaluate the longevity of eastward subduction below Mexico, and we evaluate whether the deformation history of the western North American margin in combination with the shape of the slab imaged in modern mantle structure may provide a novel first-order control on absolute North American plate motion evolution.

2. Seismic Tomography Below Mexico

The positive wave speed anomaly associated with subduction along the Central American trench (Figure 2) was one of the first anomalies interpreted as deeply subducted oceanic lithosphere (Bijwaard et al., 1998; Grand et al., 1997; Jordan & Lynn, 1974). The geometry and length of the slab changes along strike with a marked transition across the sinistral Motagua fault zone in Guatemala, which forms the western part of the Caribbean-North American plate boundary. To the north, the slab is flatter, longer, and thinner (Figure 2b) and consists of both large flat-lying and steeper segments. To the south (Figure 2a), the slab is steeper, shorter, and thicker, and flat-lying segments are largely absent. Even further north (Figure 2c), lower mantle structure is comparable to that in Figure 2b, but no anomaly is imaged in the upper ~400 km of the mantle. This is in line with the cessation of subduction at this latitude upon arrival of the Pacific-Farallon ridge in Miocene times (Atwater, 1998; Lonsdale et al., 1992). Young, hot Farallon lithosphere that subducted just before arrival of the ridge may have been partly thermally assimilated by now, which further complicates detection with seismic tomography. The length and continuity of the slab (south of Baja California) suggests long-lived, uninterrupted eastward subduction below the North American continent, which is supported by subduction modeling (Liu, 2014). This anomaly is widely known as the Farallon slab (Bijwaard et al., 1998; Grand et al., 1997), referring to the interpreted plate that this slab contains. However, in their global compilation of slabs, van der Meer et al. (2018) renamed it the Cocos slab, which was named as such after its geographic occurrence—the slab is currently connected to the Cocos Plate—to avoid tectonic interpretation in slab nomenclature. We will hereafter refer to this anomaly as the Cocos slab (van der Meer et al., 2018), but we note that its formation resulted not only from subduction of the Cocos Plate but also of Farallon lithosphere and perhaps additional plate(s) that existed in the eastern Panthalassa Ocean in Mesozoic times.

Votemaps (Shephard et al., 2017) constituting an average of seven *P* wave and seven *S* wave velocity tomography models show general agreement on the existence of an inclined positive wave speed anomaly across the entire lower mantle (Figure 2). As supporting information Movie S1 we include a video of sensitivity tests for spatial resolution (e.g., Rawlinson & Spakman, 2016) that shows sufficient detectability of the transition zone and lower mantle slab anomalies discussed here. This video also includes votemaps and mapview images of UU-P07.

3. Geological Setting

3.1. Subduction Record of Mexico

Subduction below Mexico produces and produced arc volcanism in the Trans-Mexican volcanic belt and Upper Cretaceous-Cenozoic arc magmatic provinces covering much of the continental margin of western Mexico (Ferrari et al., 2007). Older, Upper Triassic to Lower Cretaceous subduction assemblages are found in the Guerrero terrane of western Mexico and within the Alisitos arc terrane of the Baja California Peninsula (Busby et al., 1998; Campa & Coney, 1983; Figure 3). The Upper Cretaceous-Cenozoic arc complexes are widely interpreted as continental margin volcanism, but some regional paleogeographic and tectonic models postulated that the older, Triassic to Early Cretaceous assemblages were part of a large, allochthonous arc terrane that formed >1,000 km west of, and plate kinematically independent from, North America, as a result of intraoceanic subduction within the northeastern Panthalassa realm (Hildebrand, 2013; Sigloch & Mihalynuk, 2013, 2017). Field, petrological, and sedimentological studies of the Guerrero terrane have mounted evidence, however, that the Guerrero terrane is built on North American margin rocks. The terrane became temporarily separated from North America as a result of Late Jurassic to Early Cretaceous Arperos backarc basin opening, which was subsequently inverted to close in mid-Cretaceous time, all within the overriding plate of an eastward dipping subduction zone below North America (Cabral-Cano et al., 2000; Centeno-García, 2017; Centeno-García et al., 2011, 2008; Elias-Herrera et al., 2000; Martini et al., 2011). Boschman et al. (2018) recently showed that the paleolatitudinal motion of the Guerrero terrane follows North American plate motion since Early Cretaceous time, confirming the latter hypothesis.

The Guerrero arc is built upon Triassic (Carnian-Norian) sequences of turbiditic sandstones, black shales, cherts, and conglomerates containing meter-to mountain-size lenses of basalt, gabbro, chert, and limestone (Centeno-García, 2005; Centeno-García et al., 2003). The abundant turbiditic sandstones contain detrital zircons that yield Grenvillian (1.1 Ga), Pan-African (650–480 Ma), and Permian (260 Ma) U-Pb ages that match the signature of the Mexican continental mainland and the northwestern margin of the South American

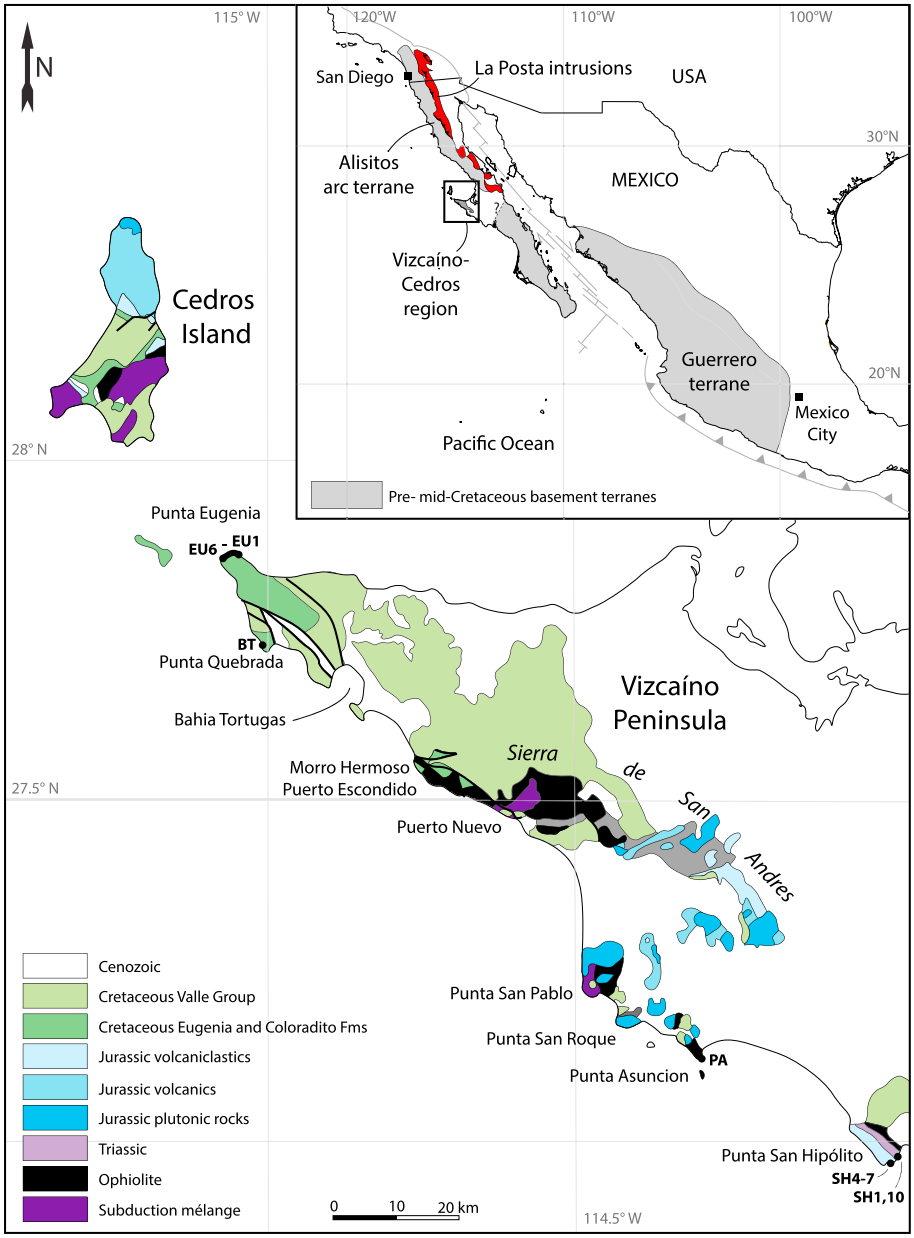

Figure 3. Geological map of the Vizcaíno Peninsula and Cedros Island, including sampling locations BT, PA, SH, and EU, modified from Kimbrough & Moore (2003). Inset: Pre-mid-Cretaceous basement terranes in western Mexico, modified from Ortega-Flores et al. (2014) and Kimbrough et al. (2006).

continent (Centeno-García et al., 2011). The Triassic sequences are intensely folded and, in some areas, metamorphosed to greenschist or amphibolite facies and are interpreted as an accretionary prism structurally overlying a subduction mélange (Centeno-García, 2005; Centeno-García et al., 1993).

The Baja California Peninsula of northwestern Mexico contains subduction records of similar age. Its basement consists of a series of northwest trending belts dominated by plutonic rocks of Cretaceous age. The peninsula became separated from the Mexican mainland and moved ~2.5° northward in late Cenozoic time during the opening of the Gulf of California, which is linked to the San Andreas transform fault system (Elders et al., 1972; Larson et al., 1968; Lonsdale, 1989; McQuarrie & Wernicke, 2005; Stock & Hodges, 1989). The peninsula consists of the Vizcaíno-Cedros region, exposing Triassic-Cretaceous subduction-related assemblages; a western belt (the Alisitos arc terrane), consisting of Lower Cretaceous volcanic, volcaniclastic, and

plutonic rocks, which intruded and overlie either continental margin or oceanic crust; and an eastern belt consisting of Upper Cretaceous *La Posta-type* plutons, which intruded in continental crust (Busby, 2004; Busby et al., 2006; DePaolo, 1981; Gastil et al., 1975; Gromet & Silver, 1987; Kimbrough et al., 2001, 2006, 2014; Premo et al., 2014; Schmidt et al., 2002, 2014; Silver & Chappell, 1988; Silver et al., 1979; Todd & Shaw, 1985; Wetmore et al., 2002, 2003). The boundary between the western and eastern belts is characterized by a series of west vergent ductile thrust faults that are locally cut by the plutons of the eastern belt, from which fault activity prior to ~99 Ma was inferred (Johnson et al., 1999; Kimbrough et al., 2001). Due to the similarities between the geological history of the Alisitos and Guerrero terranes, as well as the detrital zircon ties of both arc terranes to the North American continent, these terranes are considered to be lateral equivalents. Both arcs are underlain by a basement of Triassic-Jurassic rocks, in the Guerrero area interpreted as an accretionary prism that formed at the continental margin (Centeno-García et al., 1993, 2011; Schmidt et al., 2014; Talavera-Mendoza et al., 2007). In Early Cretaceous time, the arcs terranes separated from the continent and did not receive cratonal sedimentary detritus until after their mid-Cretaceous collision with North America (Alsleben et al., 2012; Boschman et al., 2018; Busby et al., 2006; Talavera-Mendoza et al., 2007).

3.2. Geology of the Vizcaino Peninsula

The Vizcaíno-Cedros region (Figure 3) is located along the west central coast of Baja California ~600 km south of the United States-Mexican border and exposes subduction-related rock units of Triassic to Cretaceous age (Busby, 2004; Kimbrough & Moore, 2003) that are the focus of this study. Upper Jurassic to Cretaceous forearc basin deposits of the Eugenia Formation and Valle Group are widely distributed across the Vizcaíno-Cedros region and are analogous to classic Great Valley Group forearc strata of California (Jones et al., 1976). On Cedros Island, SSZ ophiolite and arc rocks beneath this forearc cover comprise a Middle Jurassic ophiolite/arc assemblage, while on the Vizcaíno Peninsula the Upper Triassic Vizcaíno ophiolite dominates the basement. As the paleomagnetic data presented here are from rock units on the peninsula only, we limit the description of tectonic, intrusive, and stratigraphic units to the Vizcaíno Peninsula.

The main topographic feature of the Vizcaíno Peninsula is the Sierra de San Andres, an ~60-km-long east-southeast trending mountainous region with elevations up to 650 m. Limited topography in the rest of the Vizcaíno Peninsula restricts most other outcrops to the coastal areas. From structurally low to high, four units are identified: (1) a subduction mélange, (2) an ophiolite with overlying marine sediments, (3) a volcanic-plutonic complex, and (4) clastic sequences interpreted as forearc basin sediments (Barnes, 1984; Jones et al., 1976; Kimbrough, 1985; Kimbrough & Moore, 2003; Rangin et al., 1983). The structurally lowest unit of the Vizcaíno Peninsula is the Puerto Nuevo subduction assemblage: a serpentinite matrix mélange, incorporating exotic blocks of greenschist, blueschist, metagabbro, orthogneiss, amphibolite, eclogite, metabasalt, and chert. The mélange is exposed in a window in the core of an antiform forming the western part of the Sierra de San Andres (Moore, 1986).

Structurally overlying is the Upper Triassic Vizcaíno ophiolite, cropping out in the northwestern part of the Sierra de San Andres and in some isolated exposures along the coast from Punta Quebrada in the north to Punta San Hipólito in the south. The most complete ophiolitic section is exposed in the Sierra de San Andres, where the ophiolite forms a west plunging antiform and exposes serpentinized harzburgite-dunite tectonite, gabbro, dykes, sills, and pillow basalts with a total estimated thickness of 3 km (Kimbrough & Moore, 2003). Other, more dismembered ophiolite sections vary from exposing gabbro, sheeted dykes, and pillow lavas (Punta Asuncion) to only pillow lavas (Punta San Hipólito; Figure 3). The ophiolite is dated by radiolaria in interpillow limestones at Punta Quebrada and near Morro Hermoso (Carnian to upper to middle Norian, ~237–215 Ma; Barnes, 1984), by sphene U-Pb dating of a gabbro dyke in the northern flank of the antiform of the Sierra de San Andres (220 ± 2 Ma; Barnes & Mattison, 1981) and by zircon U-Pb dating of a plagiogranite in the southern flank (221 ± 2 Ma; Kimbrough & Moore, 2003). Based on geochemical analysis, the Vizcaíno ophiolite is interpreted to have formed in a SSZ setting (Moore, 1983, 1985). The magmatic ophiolite section is conformably overlain by siliceous and pelagic sediments of Norian to Early Jurassic age. The cover of the Sierra de San Andres ophiolite is a 200- to 300-m section of vitric tuffs, tuffaceous chert, sandstone, and limestone (Barnes, 1984). These sediments are correlated with a thin sequence of pink dolomite and red chert overlying the pillows at Punta Quebrada and with a 2,400-m-thick sequence of green chert, limestone, breccia, and sandstone at Punta San Hipólito (Barnes, 1982, 1984; Finch & Abbott, 1977).

Intruding and overlying the ophiolitic basement is an Upper Jurassic arc volcanic-plutonic complex, mainly cropping out in the southeastern part of the Sierra de San Andres and around San Pablo and San Roque. The complex contains gabbroic-to-granodioritic intrusions, andesite lavas, and breccia and pillow lavas, interbedded with volcaniclastic sandstone, conglomerate, and breccia (Kimbrough & Moore, 2003). K-Ar (hornblende, biotite) and U-Pb (zircon) ages from plutonic rocks range from ~160 to 135 Ma (Barnes, 1982, 1984; Kimbrough & Moore, 2003; Torres-Carrillo et al., 2016; Troughton, 1974). The volcanic rocks in the Sierra de San Andres have island arc tholeiitic and boninitic geochemical affinities (Moore, 1983), and the volcaniclastic rocks are interpreted as proximal coarse-grained debris aprons deposited along a steep volcanic slope (Moore, 1984).

The sedimentary Eugenia Formation consists of Tithonian-Valanginian (Barnes, 1984) marine volcanogenic strata intercalated with local pillow lavas and major sedimentary olistostrome intervals with megablocks of Triassic chert and Paleozoic sandstone (Kimbrough & Moore, 2003). It is in depositional contact with the Vizcaíno ophiolite and its sedimentary cover (Kimbrough & Moore, 2003). A tuff within the Eugenia Formation at the northern tip of the Vizcaíno Peninsula is dated at 141.5 ± 3 Ma (Hickey, 1984), which is within the age range of the plutons of the Sierra de San Andres arc, suggesting that the strata of the Eugenia Formation are derived from the arc volcanoes of the Sierra de San Andres volcanic-plutonic complex (Barnes, 1984; Minch et al., 1976; Rangin, 1978). The Eugenia Formation is interpreted to have formed in a basin that collected active arc volcaniclastic debris as well as erosional material from exposed basement at topographic highs on the edges of the basin (Kimbrough & Moore, 2003). Detrital zircon U-Pb ages from Eugenia Formation strata document significant components of Appalachian-derived Paleozoic (480–300 Ma), Pan African (641–531 Ma), and Grenville (1335–950 Ma) grains that indicate along-strike correlation of the Vizcaíno forearc to the Great Valley Group of California and indicate deposition within the same west facing arc system (Kimbrough et al., 2014).

Overlying the Eugenia Formation are the widely exposed Aptian-Albian to Eocene, dominantly deep-marine strata of the Valle Group, interpreted as forearc basin turbidites (Busby-Spera & Boles, 1986; Kimbrough et al., 2001, 2006; Patterson, 1984; Smith & Busby, 1993).

Many authors have interpreted the Vizcaíno-Cedros ophiolite and arc complexes as allochthonous intraoceanic terranes that accreted to the North American margin by Late Jurassic time, formed either above a Triassic-Jurassic westward dipping (Boles & Landis, 1984; Busby-Spera, 1988; Critelli et al., 2002; Sigloch & Mihalynuk, 2017) or eastward dipping subduction zone (Barnes, 1984; Rangin, 1978). However, based on the absence of a Triassic intraoceanic arc, an accretionary prism or crustal suture east of the ophiolite, as well as the lack of evidence of major crustal shortening or a collision, Kimbrough and Moore (2003) instead argued that forearc rifting models developed for the Californian ophiolite belt to the north (Saleeby, 1981, 1992; Stern & Bloomer, 1992) may better explain the formation of the Vizcaíno-Cedros ophiolite and arc complexes.

4. Sampling Locations and Ages

We collected a total of 233 cores and 41 hand samples from four different locations. Our sampling strategy aims at sufficiently sampling paleosecular variation (PSV) per locality. Pillows from the Vizcaíno ophiolite were sampled in two locations, at Punta Asuncion (PA1-4, 44 cores from a coastal exposure of ~350 m; Figure 4a) and at Bahia Tortugas (BT, 19 cores from an ~30-m exposure; Figure 4b). To maximize the amount of geological time in our sample collection of the ophiolite, all samples were collected from individual pillows at least a few meters apart. Samples were collected from the center of the pillows. Interpillow limestones at Bahia Tortugas contain Norian radiolaria (Barnes, 1984). The pillows at Punta Asuncion are not dated, but there is close agreement on the age of formation of the ophiolite from different outcrop locations (Kimbrough & Moore, 2003). Therefore, we assign all ophiolitic pillows to the same Norian (221 ± 2 Ma) age interval. Paleohorizontal was determined per site by averaging multiple measurements of bedding of interpillow sediments, as well as estimates of paleohorizontal from pillow geometry.

Second, we sampled the sedimentary cover of the ophiolite at Punta San Hipólito (SH; 41 hand samples of green chert [SH1–SH3, SH8–SH11, sampled through ~150 and ~100 m of stratigraphy, respectively; Figures 4c and 4d) and 31 cores of fine-grained sands and cherty clays (SH4–SH7, 38 cores from an ~300-m exposure, Figure 4e). Samples were taken in stratigraphic order and ~2–5 m of stratigraphic thickness was sampled per site. The green cherts are from the up to 245-m-thick lowermost member of the San Hipólito Formation, deposited directly on top of the basal pillows (Finch & Abbott, 1977). The cherts

Figure 4. Field photographs. (a) Pillow lavas at Punta Asuncion (PA1). (b) Pillow lavas at Punta Quebrada, near Bahia Tortugas, size of exposure on photo: ~5 m. (c, d) Chert member of the San Hipólito Formation (SH10 and SH1), stratigraphic thickness of chert beds in d: ~40 cm. (e) Sandstone member of the San Hipólito Formation (SH5). (f) Eugenia Formation (EU6), stratigraphic thickness of sandstone beds: ~4 m.

contain middle Norian radiolaria (Pessagno et al., 1979; Whalen & Pessagno, 1984). The upper 1,840 m of the San Hipólito Formation is occupied by the sandstone member (Finch & Abbott, 1977) of which we sampled resistant fine grained sands and cherty clays. We sampled the lowermost part of this member, which contains Lower Jurassic (upper Pliensbachian to Toarcian) radiolaria (Whalen & Pessagno, 1984).

Third, we sampled the Eugenia Formation at Punta Eugenia (EU, 139 samples, distributed over six sites through the succession [sampled in stratigraphic order on the site, as well as location level] with a total stratigraphic thickness of ~3 km; Figure 4f). Per site, 5–15 m of stratigraphic thickness was sampled. Rocks at site EU6 were dated at 141.5 ± 3 Ma by U/Pb on zircon (Hickey, 1984); the rest of the samples were collected at stratigraphically lower levels.

5. Methods

Typical paleomagnetic cores, 2.5 cm in diameter, were sampled with a gasoline-powered motor drill. Their orientation was measured with an ASC OR-2 orientation device and Brunton compass. Oriented hand samples were taken when the rock was too hard to drill in the field, and for these samples two or three cores per hand sample were drilled in the laboratory using a drill press. Using a double blade circular saw, the cores were cut into samples of 2.2-cm length. Laboratory analyses were carried out at the Paleomagnetic Laboratory Fort Hoofddijk of Utrecht University, the Netherlands. To determine the nature of the magnetic carriers, thermomagnetic analyses were performed on representative samples for each locality, using a horizontal translation-type Curie Balance with cycling applied magnetic field of 100–300 or 250–300 mT (Mullender et al., 1993). In order to detect magneto-mineralogical alterations during heating, a number of heating-cooling cycles was applied. We used the following temperature scheme (in degrees Celsius): 20–150, 50–250, 150–350, 250–400, 350–450, 350–500, and 400–700. All samples were subjected to either alternating field (AF) or stepwise thermal demagnetization, and the natural remanent magnetizations were

measured on a 2G DC SQUID cryogenic magnetometer. Demagnetization steps used were 4, 8, 12, 16, 20, 25, 30, 35, 40, 45, 50, 60, and 80 mT for AF treatment and variable temperature increments up to 600 °C for thermal treatment. AF treatment demagnetization was performed on an in-house developed robotized demagnetization device (Mullender et al., 2016). We plotted demagnetization diagrams on orthogonal vector diagrams (Zijderveld, 1967) and determined the magnetic components via principal component analysis (Kirschvink, 1980). When applicable, we performed the fold test of Tauxe and Watson (1994) and to test for common means between two data sets, the bootstrapped coordinate test of Tauxe (2010). Following statistical procedures described in Deenen et al. (2011), we calculated mean directions using Fisher (1953) statistics on virtual geomagnetic poles and applied a 45° cutoff to the virtual geomagnetic poles per locality (Johnson et al., 2008). Sample interpretation and statistical analysis were operated in the online portal Paleomagnetism.org (Koymans et al., 2016). The supporting information contains all paleomagnetic results, which may be imported and viewed in the portal.

6. Paleomagnetic Data Compilation

We compiled all previously published paleomagnetic data from the Vizcaíno-Cedros region (Data Set S1). Because the purpose of our study is to test the plate tectonic affinity of the Vizcaíno ophiolite and arc complexes, we restrict our data compilation to the ophiolite and the overlying sediments and arc magmatic rocks. We thus do not include paleomagnetic data from rocks in the subduction mélange on Cedros Island derived from lithosphere that subducted below the ophiolite. Papers with paleomagnetic data generally provide only site averages and their statistical parameters (N, k, and α_{95}), and not the original directions per sample. In volcanic rocks, acquisition of the natural remanent magnetization occurs geologically instantaneously upon cooling, and therefore, theoretically, all samples from a single lava flow yield the same paleomagnetic direction. Therefore, using site averages for volcanic rocks is not problematic. However, for sedimentary or slowly cooling intrusive igneous rocks, different samples from one site represent (slightly) different geological ages. Therefore, these sites include a certain amount of PSV and it is preferred to perform statistics on the actual distribution of individual directions rather than on site averages that do not take this PSV into account (Deenen et al., 2011). To allow for this, we created parametrically sampled data sets for sites of intrusive or sedimentary rocks using the online portal Paleomagnetism.org (Koymans et al., 2016). As the result of parametrical sampling, our mean directions may differ from the originally published means. However, this deviation in declination and inclination is never larger than 3°.

For the paleomagnetic database, we selected data according to the following quality criteria: (1) the total distribution of directions satisfies the quality criteria of representing PSV (i.e., $A_{95min} < A_{95} < A_{95max}$; Deenen et al., 2011) and (2) sedimentary and intrusive igneous rocks have $n \geq 4$, lavas have $k \geq 50$ (Biggin et al., 2008; Johnson et al., 2008), and at least seven lava sites could be averaged from a locality. Sites discarded by the original authors were not taken into account, if reasons were provided (e.g., remagnetization).

7. Paleomagnetic Results

7.1. Vizcaíno Ophiolite Pillow Lavas: Bahia Tortugas (BT) and Punta Asuncion (PA)

Curie temperature of the BT and PA pillow lavas is close to 580° (Figures 5a and 5b), indicating that the magnetic carrier in the samples is magnetite. Demagnetization diagrams reveal a minor overprint at steps up to 10 mT or 150 °C and linear decay toward the origin at temperatures up to 580 °C. Characteristic Remanent Magnetizations (ChRMs) were generally interpreted at high temperatures (~450–600 °C) or ~25–50 mT (Figures 5c–5g). Initial intensities range from 8 to 2,000 mA/m. When corrected for bedding tilt, directions from BT and PA are antipodal and share a Common True Mean Direction (CTMD). Variations in bedding orientation allow for a fold test, which is positive (best fit between 53% and 117% unfolding; Figure 5i). Inclinations are consistently shallow, declinations are large, and there is no control on hemispheric origin or direction (clockwise or counterclockwise) of rotation. Furthermore, both normal and reversed polarities are common within the 221 ± 2-Ma interval during which the rocks were formed (Gradstein et al., 2012). Therefore, there are two possible solutions representing paleolatitudes just north or just south of the equator, with opposite rotations. Clockwise declinations are in line with directions from SH4–SH7 and declinations from the San Roque pluton reported by Torres-Carrillo et al. (2016; see below), which we therefore consider the most likely option. We reversed the polarity of PA1-4, and we combined the directions of both localities for the

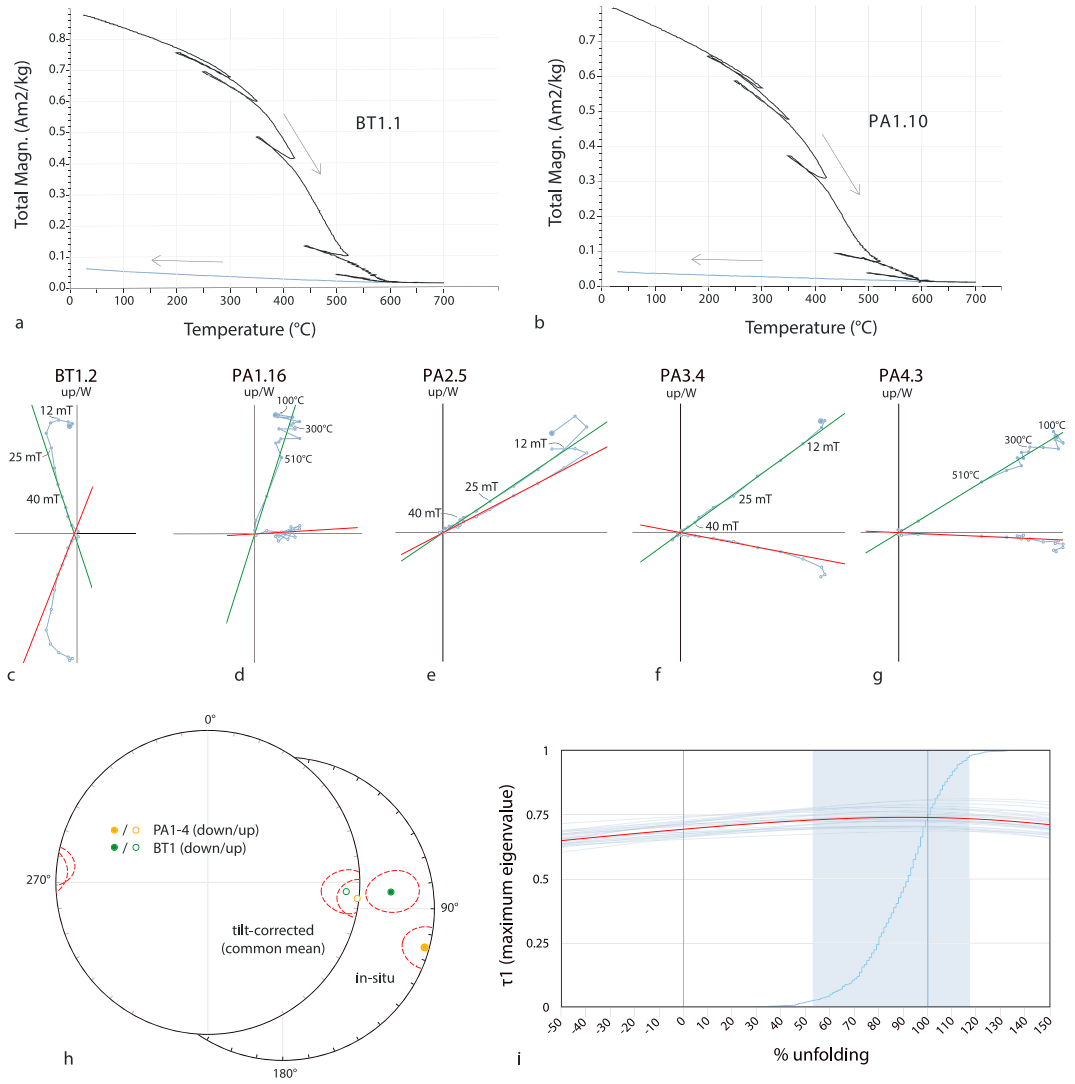

Figure 5. Rock magnetic and paleomagnetic results from localities PA and BT. (a, b) Thermomagnetic curves measured on a Curie balance. Heating in black, cooling in blue. (c–g) Orthogonal vector diagrams in geographic coordinates, closed (open) symbols for projection on a horizontal (vertical) plane. (h) Mean directions of PA1–PA4 and BT, including confidence intervals (red dashed lines) in both geographic and tectonic coordinates. PA1–PA4 have been inverted. (i) Bootstrapped fold test: cumulative distribution function (with confidence interval in light blue) based on 1,000 bootstraps (average of bootstraps in red).

calculation of a single paleomagnetic pole (Figure 5h). There are three lines of evidence that support the primary nature of the magnetization: (1) the fold test is positive, supporting pretilt magnetization acquisition, (2) the directions in both geographic and tectonic coordinates differ significantly from the GAD field direction, and (3) the distribution of the ChRMs satisfies the quality criteria of representing PSV (i.e., $A_{95min} = 2.4 < A_{95} = 5.7 < A_{95max} = 6.6$; Deenen et al., 2011). The average (tilt-corrected) ChRM direction is Dec ± ΔD_x = 95.5 ± 5.7°, Inc ± ΔI_x = −3.8 ± 11.4°, n = 54, K = 12.4, and A_{95} = 5.7 (Table 1).

7.2. Vizcaíno Ophiolite Sedimentary Sequence: San Hipólito Formation (SH)

The two sampled members of the San Hipólito Formation (the chert member [SH1 and SH10] and the sandstone member [SH4–SH7]), yield very different demagnetization results. Curie temperatures of the chert member (SH1 and SH10) are 540–560° (Figure 6a), indicating that the magnetic carrier is magnetite. Initial intensities were very low: 0.2–50 mA/m, and ChRMs were interpreted at midrange temperatures (180–480 °C; Figures 6c, 6h, and 6i). The sampled strata did not vary significantly in bedding orientation, and the

Table 1
Paleomagnetic Results

Localities	N	N_{45}(is)	N_{45}(tc)	In situ D	In situ ΔD_x	In situ I	In situ ΔI_x	Tilt corrected D	Tilt corrected ΔD_x	Tilt corrected I	Tilt corrected ΔI_x	k	α_{95}	K	$A_{95min} < A_{95} < A_{95max}$	
EU1–6	128	127		197.8	1.6	39.2	2.1					*63.5*	*1.6*	*70.3*	*1.7 > 1.5 < 3.9*	a
SH4–SH7	38	34	34	167.0	4.7	45.4	5.2	178.3	3.4	15.0	6.3	33.0	4.4	55.9	2.9 < 3.3 < 8.9	
SH4–SH7 corrected	38	34	34	167.0	4.7	45.4	5.2	178.3	3.4	24.0	6.3	33.0	4.4	55.9		
SH1 and SH10	36	36		348.0	3.9	43.7	4.5					*54.0*	*3.3*	*48.1*	*2.9 < 3.5 < 8.6*	a
BT1	19	14	15	81.4	10.6	28.3	17.1	93.8	9.0	−9.6	17.6	11.5	11.8	19.1	4.1 < 9 < 14.9.0	
PA1–PA4	44	40	39	284.7	7.7	−2.7	15.4	277.3	6.9	3.2	13.8	8.0	8.7	11.9	2.8 < 6.9 < 8.2	
All pillow lavas	63	54	54	97.4	7.2	11.6	13.9	95.5	5.7	−3.8	11.4	8.1	7.2	12.4	2.4 < 5.7 < 6.6	

Note. N: number of demagnetized specimens; N_{45}(is)/N_{45}(tc): number of specimens that fall within the 45° cutoff in in situ coordinates/after tilt correction. D: declination; I: inclination. SH4–SH7 corrected: inclination corrected for inclination shallowing by applying compaction factor 0.6.
[a]Statistical values on in situ directions.

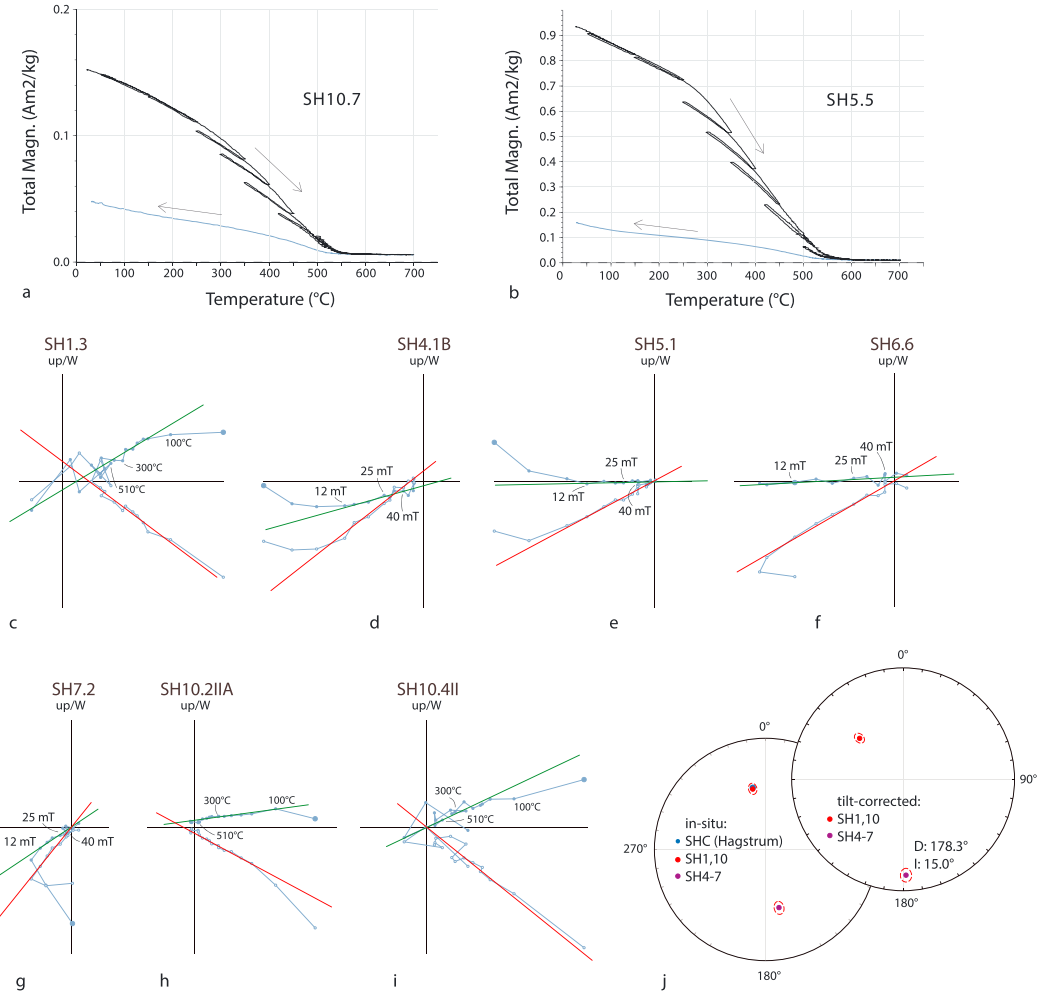

Figure 6. Rock magnetic and paleomagnetic results from locality SH. (a, b) Thermomagnetic curves measured on a Curie balance. Heating in black, cooling in blue. (c–i) Orthogonal vector diagrams in geographic coordinates, closed (open) symbols for projection on a horizontal (vertical) plane. (j) Mean directions, including confidence intervals (red dashed lines) of SH1 and SH10, SH4–SH7, and SHC of Hagstrum et al. (1985), in both geographic and tectonic coordinates.

demagnetization experiments yielded normal directions only. Therefore, neither the fold nor the reversal test can be performed. However, the San Hipólito chert member was also sampled by Hagstrum et al. (1985; their sites SHC1 and SHC2; results reevaluated in Hagstrum et al. 1993). Based on a negative fold test from the overlying limestone member, Hagstrum et al. (1993) concluded that the San Hipólito section acquired its magnetization after folding. Our chert member mean direction is statistically indistinguishable from the SHC mean direction of Hagstrum et al. (1993) in geographic coordinates (before bedding tilt correction; Figure 6j). Therefore, we consider it most likely that the directions obtained from SH1 and SH10 represent a posttilting remagnetization. The average (in situ) ChRM direction is Dec ± ΔD_x = 348.0 ± 3.9°, Inc ± ΔI_x = 43.7 ± 4.5°, n = 36, K = 48.1, and A_{95} = 3.5 (Figure 6j). Assuming that these strata were not affected by a second folding or tilting event, this inclination corresponds to a paleolatitude 25.6°N (ranging 22.2–29.2°N), which is within range of paleolatitudes of the Vizcaíno-Cedros region from the Eocene to present as predicted by the Global Apparent Polar Wander Path (GAPWaP; Torsvik et al., 2012; Figure 8), suggesting that remagnetization occurred sometime during this interval.

Curie temperatures of the sandstone member (SH4–SH7) are close to 580 °C (Figure 6b), indicating that the magnetic carrier in the samples is magnetite. Initial intensities range from 5 to 550 mA/m, and ChRMs were interpreted at ~150–540 °C or ~16–60 mT (Figures 6d–6g). Again, no field tests were possible to determine the nature of the magnetization and both the distributions of ChRMs in both geographic and tectonic coordinates satisfy the quality criteria of representing PSV (i.e., $A_{95min} < A_{95} < A_{95max}$). Despite this, we consider a primary origin of the magnetic signal likely, for the following reasons. In geographic coordinates, the declinations of SH4–SH7 differ 180° from the SH1 and SH10 directions that carry a posttilt magnetization (Figure 6j), yet have positive inclinations, both in geographic and tectonic (tilt-corrected) coordinates, suggesting that the SH4–SH7 directions reflect a rotated normal component rather than a reversed component. This difference cannot be explained by a postremagnetization vertical axis rotation of SH4–SH7, as all San Hipólito samples are collected throughout a continuous stratigraphic succession with uniform bedding orientations. Furthermore, the strongly rotated declinations found in SH4–SH7 cannot be acquired during a younger remagnetization event, since that would require them to be present in SH1 and SH10 as well. This indicates that the magnetization of SH4–SH7 predates the remagnetization of SH1 and SH10 and is, in the absence of any indication of a second remagnetization event, most likely primary. The average ChRM (tilt-corrected) direction is Dec ± ΔD_x = 178.3 ± 3.4°, Inc ± ΔI_x = 15.0 ± 6.3°, n = 34, K = 55.9, and A_{95} = 3.3 (Figure 6j). We correct for inclination shallowing, typical in fine grained clastic rocks, by applying a standard compaction factor of 0.6 (Torsvik et al., 2012), which increases the average inclination from 15.0° to 24.0°, yielding a paleolatitude of 12.6°N (Figure 8).

7.3. ForeArc Sedimentary Sequence: Eugenia Formation (EU)

Curie temperatures of the EU sediments are 580 °C (Figure 7a), indicating that the magnetic carrier in the samples is magnetite. ChRMs were isolated at midrange temperatures (~210–390 °C) or alternating fields (~16–45 mT; Figures 7b–7g). Initial intensities range from 2 to 11 mA/m. Variations in bedding orientation between the six sites allow for a fold test, which is negative (best fit between −42% and −5% unfolding; Figure 7h). Furthermore, the A_{95} calculated in geographic coordinated (1.5°) falls below the A_{95min} = 1.7°, indicating low dispersion, which suggests remagnetization. The average (in situ) ChRM direction is Dec ± ΔD_x = 197.8 ± 1.6°, Inc ± ΔI_x = 39.2 ± 2.1°, n = 127, K = 70.3, and A_{95} = 1.5 (Figure 7i). Again, the associated paleolatitude (22.2°N, ranging 20.7–23.7°N) is within range of paleolatitudes of the Vizcaíno-Cedros region during the last 50 Myr as predicted by the GAPWaP (Torsvik et al., 2012; Figure 8).

7.4. Paleolatitudinal History of the Vizcaíno Peninsula

To test whether the Vizcaíno ophiolite has moved coherently with the North American Plate, we compute the GAPWaP of Torsvik et al. (2012) in coordinates of Baja California using Euler poles for Baja California relative to North America computed from the reconstruction of McQuarrie and Wernicke (2005) following procedures described in Li et al. (2017). To compute Euler rotations for Baja California relative to North America, we have recreated the ArcGIS-based model of McQuarrie and Wernicke (2005) in GPlates plate reconstruction software (supporting information). Except for two of the nine Upper Cretaceous sedimentary sites (Patterson, 1984), all previously published and new paleomagnetic data from the Vizcaíno-Cedros region yield paleolatitudes equal to the expected paleolatitudes of Baja California when corrected for Gulf of California opening (Figure 8a). Discordance of the two Cretaceous sites may be explained by inclination shallowing due to compaction in sedimentary rocks (Tauxe & Kent, 2004). Furthermore, declinations of >90° in Jurassic and Triassic

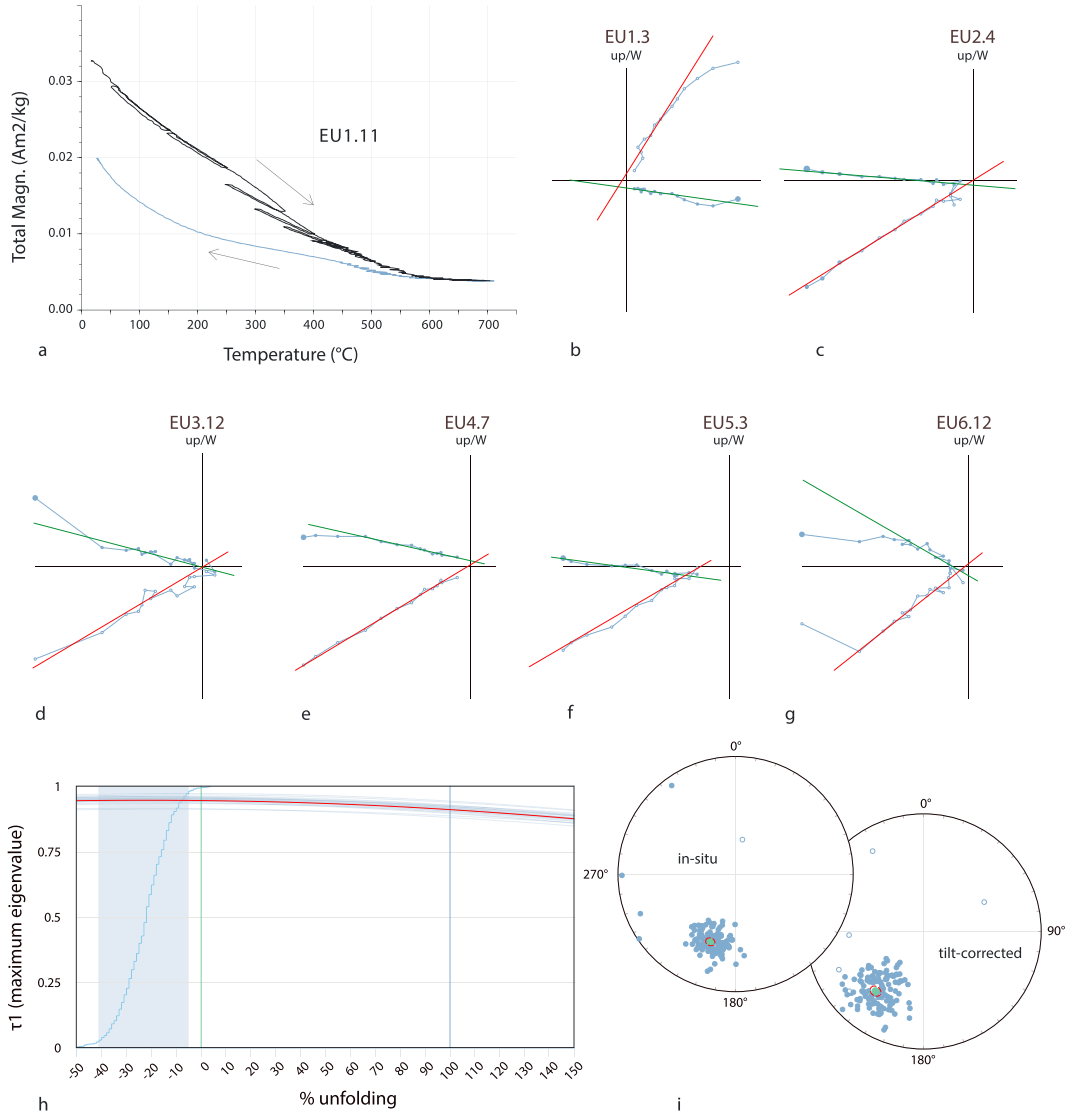

Figure 7. Rock magnetic and paleomagnetic results from locality EU. (a) Thermomagnetic curve measured on a Curie balance. Heating in black, cooling in blue. (b–g) Orthogonal vector diagrams in geographic coordinates, closed (open) symbols for projection on a horizontal (vertical) plane. (h) Bootstrapped fold test: cumulative distribution function (with confidence interval in light blue) based on 1,000 bootstraps (average of bootstraps in red). (i) Directions (in blue), means (in green), and their confidence intervals (red dashed lines) of locality EU, both in geographic and tectonic coordinates.

sites suggest pre-Cretaceous clockwise vertical axis rotations (Figure 8b), which may best be explained by local vertical axis rotations close to the oblique subduction plate boundary.

8. Discussion

8.1. 220 Myr of Subduction Below Mexico

SSZ zone ophiolites, such as the Vizcaíno ophiolite, are widely interpreted to form in forearc settings during the subduction initiation process (e.g., Stern et al., 2012; Wakabayashi et al., 2010), or shortly thereafter, during the first stage of overriding plate extension following subduction initiation (van Hinsbergen, Peters, et al., 2015). They may form both in intraoceanic settings (e.g., Philippine Sea plate; Stern & Bloomer, 1992) or Neotethys (Dilek & Furnes, 2011; Maffione et al., 2017; Maffione & van Hinsbergen, 2018; Maffione, van Hinsbergen, et al., 2015; Moix et al., 2008), as well as along or close to continental margins (e.g., the

Californian Coast Range Ophiolite; Metcalf & Shervais, 2008; Shervais et al., 2004; Wakabayashi, 2015), the Indus-Yarlung ophiolites of Tibet (Huang et al., 2015; Maffione, Thieulot, et al., 2015; Pozzi et al., 1984), or the Izmir-Ankara ophiolites of northern Turkey (Topuz, Çelık, et al., 2013; Topuz, Göçmengil, et al., 2013).

Our new paleomagnetic data from the Vizcaíno-Cedros region yield a paleolatitudinal plate motion history equal to that of the North American Plate since Late Triassic time. We follow the argumentation of Boschman et al. (2018) on the kinematic relationship between the Guerrero terrane and North America: latitudinal (northward) plate motion relative to the North American continent is expected for an accreted exotic terrane that formed in an intraoceanic setting on one of the oceanic plates of the eastern Panthalassa Ocean (e.g., Farallon, Kula). A latitudinal plate motion history equal to that of the North American Plate, on the other hand, indicates that the "accreted" terrane formed within the (deforming by forearc or backarc spreading and subsequent shortening) upper plate. We therefore interpret that the Vizcaíno-Cedros rock assemblages formed within the North American upper plate and were located above an eastward dipping subduction zone consuming oceanic lithosphere of the eastern Panthalassa Ocean. Triassic forearc spreading created oceanic crust in the North American forearc, thereby widening the gap between the trench and the continental margin. As a result, the volcanic arc developed west of the continental margin, on oceanic and/or stretched accretionary prism basement.

The ~220-Ma Vizcaíno SSZ ophiolite marks the minimum age of onset of subduction of Panthalassa lithosphere forming the Cocos slab, which has been subducting ever since. This inference has several first-order implications. First, it shows that the longest still-subducting slab is also the oldest, even older than previously estimated by van der Meer et al. (2018) who assigned an ~170 Ma age based on correlation to Californian geological records. Second, it shows that there has been direct interaction between the Panthalassa plate system and the Pangea-related plates since at least 220 Ma. The inferred east dipping continental margin subduction in Mexico is consistent with the record of earliest Cordilleran magmatism along strike to the north in the southwestern United States recorded by Triassic plutons (218–213 Ma) that intrude Proterozoic cratonal basement (Barth et al., 1997). Triassic magmatism in both regions was also followed by a magmatic lull before onset of voluminous Middle to Late Jurassic arc magmatism.

8.2. Paleolatitudes in a Mantle Reference Frame

We have shown that the Mexican geological record of subduction may be correlated to (>)220 Myr of subduction below North America. However, before correlating this record to interpret the modern structure of the Cocos slab, we first need to test whether North America did not undergo major latitudinal changes relative to the mantle in this time interval. If that is the case, then the records of Mexico may (in part) belong to slab remnants located in the mantle to the north or south of the Cocos slab. Figure 8 illustrates that in a paleomagnetic reference frame (so relative to the Earth's spin axis), the North American Plate underwent little latitudinal motion throughout the Late Cretaceous and Cenozoic but shows a >30° northward shift during the Late Triassic and Jurassic (Figures 8 and 9) followed by an ~10° southward shift in the Early Cretaceous (Torsvik et al., 2012). Other paleomagnetic reference frames (Besse & Courtillot, 2002; Kent & Irving, 2010) show a similar movement. However, to correlate North American plate kinematic history to mantle structure, these latitudes should first be converted to a mantle reference frame, thereby switching from plate motions relative to the spin axis to plate motions relative to the lower mantle, filtering out contributions of True Polar Wander (TPW) to apparent polar wander (Steinberger & Torsvik, 2008; Torsvik et al., 2012; see also van Hinsbergen, de Groot, et al., 2015). Differences between the paleomagnetic reference frames with and without correction for TPW (shaded areas in Figure 9) represent two well-known TPW events in Cretaceous and Jurassic times (Steinberger & Torsvik, 2008; Torsvik et al., 2012). From Figure 9 it follows that since 190 Ma, the Vizcaíno Peninsula (now at ~28°N) has been between 25°N and 35°N, implying that correlating the Mexican geological subduction records to mantle structure at these same latitudes is warranted. In Late Triassic to Early Jurassic time, the North American Plate moved ~15° to the north relative to the mantle (Figure 9), which may imply that the oldest, Upper Triassic geological records of subduction (at the North American Plate) may be offset relative to deep mantle structure by such a distance, assuming that the slab did not undergo lateral dragging (Spakman et al., 2018), which may offset slabs relative to their initial position of subduction laterally by >10° (Van de Lagemaat et al., 2018). We also note that the TPW calculations of Steinberger and Torsvik (2008) and Torsvik et al. (2012) include a mantle-fixed TPW-Euler pole that pierces through the centers of mass of the Large Low Shear wave Velocity Provinces at the core-mantle boundary.

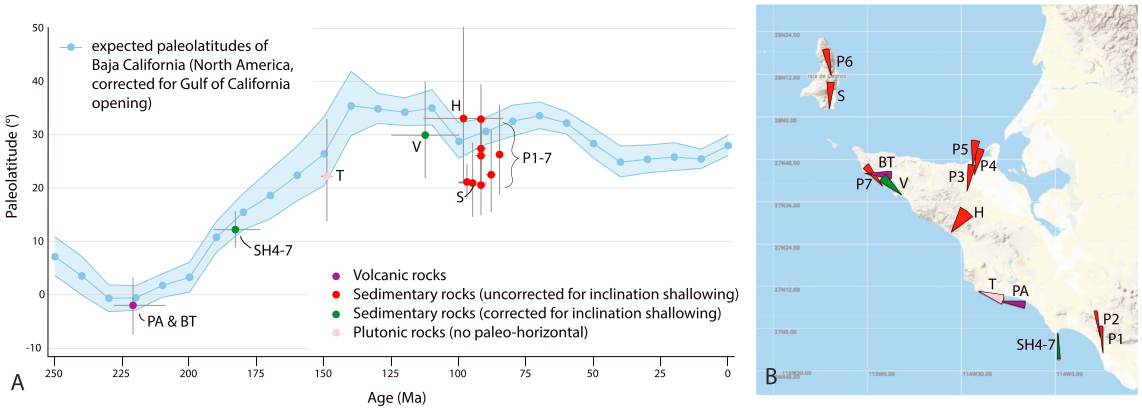

Figure 8. Paleomagnetic database of the Vizcaíno-Cedros region, including data from Hagstrum et al. (1985; H), Patterson (1984; P1–P7), Smith and Busby (1993; S), Torres-Carrillo et al. (2016; T), Vaughn et al. (2005; V), and this study (SH4–SH7, PA, and BT). (a) Paleolatitudes. The data are plotted with respect to the expected paleolatitudes of Baja California (blue), calculated for a reference location within the Vizcaíno Peninsula (chosen at 27.4°N, −114.4°W). We use the reference values predicted by the Global Apparent Polar Wander Path of Torsvik et al. (2012). The paleolatitudinal path of Baja California differs from North America, as we correct for Neogene Gulf of California opening following the reconstruction of McQuarrie and Wernicke (2005). (b) Sampling locations and declinations with confidence parachutes (ΔD_x).

Shifting the Indo-Atlantic plate system westward relative to the mantle, for example, through slab fitting (van der Meer et al., 2010), thus requires recalculating TPW at each step (Torsvik et al., 2014), potentially shifting the TPW-corrected paleolatitudes. For simplicity, in the following correlation between overriding plate and subducted slab, we do not take latitudinal overriding plate motion and iterative TPW recalculation into account and use a single cross section through the Cocos slab, noting that this may add uncertainty to the pre-190-Ma correlation.

8.3. Slab Geometry and Absolute Plate Motions

The Cocos slab anomaly contains a steep thickened segment between ~1,000 and 1,800 km and two low-angle, partially flat slab segments, one in the upper mantle and one in the uppermost lower mantle above ~1,000 km. In the upper mantle and below 1,800 km, the anomaly dips eastward. These geometry variations

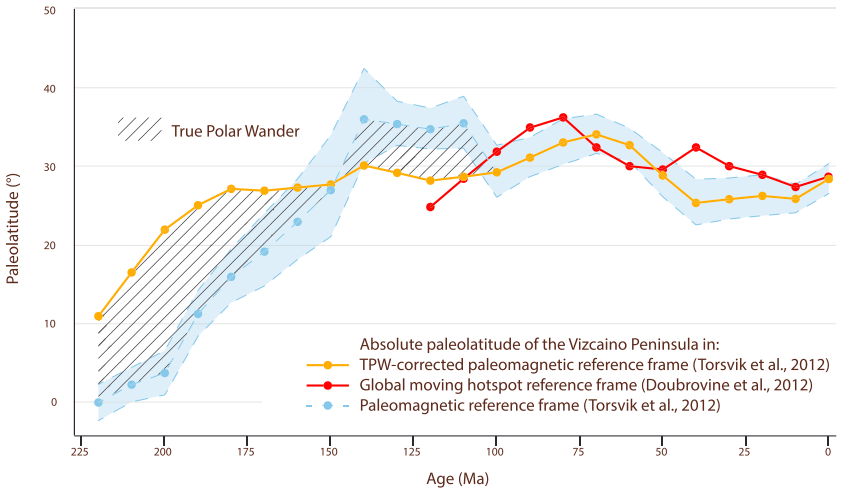

Figure 9. Absolute paleolatitudinal plate motion of the North American Plate at the latitude of the Vizcaíno Peninsula trough time, based on (1) on the global moving hot spot reference frame of Doubrovine et al. (2012) in orange, (2) the paleomagnetic reference frame corrected for True Polar Wander of Torsvik et al. (2012) in red, and (3) the paleomagnetic reference frame of Torsvik et al. (2012) in blue. Reference frames (1) and (2) represent paleolatitudinal plate motion relative to the lower mantle, whereby the difference between the red and orange lines provides an implicit measure for uncertainties in the methods and data used to establish these mantle reference frames. Shaded areas represent True Polar Wander.

suggest episodes of subduction associated with mantle-stationary subduction alternated with episodes of westward rollback. We now analyze the interplay between upper plate deformation as recorded in Mexican geology since the Triassic, absolute plate motions of the North American Plate, motions of the slab relative to the mantle, and development of the complex geometry of the Cocos slab. We build upon the concepts recently introduced by Schepers et al. (2017) for subduction below the Andes: we use the absolute motion of the *slab bend* (SB in Figure 10), that is, the location where the subducting plate (PAN) changes from (sub)horizontal to dipping into the mantle (M) as a measure for slab rollback. The state of stress and related deformation in the Mexican continental margin is the result of the relative motion between the overriding plate (NAM) and the trench (T): net divergence (convergence) between the trench and the overriding plate generates overriding plate extension (shortening) (Heuret & Lallemand, 2005; Lallemand et al., 2005; Schellart, 2008a, 2008b). Subduction occurring with a mantle-stationary slab bend leads to formation of near-vertical, thickened piles of subducted material, termed *slab walls* by Sigloch and Mihalynuk (2013). An example of a still-subducting mantle-stationary slab is the Marianas slab that subducts steeply into the lower mantle (Miller et al., 2005; van der Meer et al., 2018). When a slab rolls back, that is, the slab bend migrates relative to the mantle in the direction of the subducting plate, slabs tend to horizontally drape the 660-km discontinuity (Faccenna et al., 2001; Funiciello et al., 2004; van der Hilst & Seno, 1993), with well-known examples in the western Mediterranean region (Faccenna et al., 2004; Spakman & Wortel, 2004), the Banda slab (Spakman & Hall, 2010), the Izu-Bonin slab (Miller et al., 2005; van der Meer et al., 2018), or the Tonga slab (Bijwaard et al., 1998; Hall & Spakman, 2002; van der Hilst, 1995). We note the paradox in slab geometry between the uppermost and mantle transition zone here: subduction with a mantle stationary slab bend and an advancing overriding plate, a situation that may generate flat slab subduction, corresponds to the formation of vertical slab walls in the mantle transition zone, whereas steep subduction (and rollback) corresponds to slabs draping the base of the upper mantle, forming horizontal slab segments in the mantle transition zone. In other words, the flat and steep anomaly segments in modern mantle structure correspond to phases of ancient steep and flat slab subduction, respectively.

Correlation of Cocos slab geometry with the geological record of the deformed western margin of Mexico may provide constraints on the timing of formation of the flat and steep segments. We define the following first-order states of overriding plate deformation: (1) Late Triassic oceanic forearc spreading, forming the Vizcaíno ophiolite's crust; (2) no major deformation in latest Triassic to latest Jurassic time; (3) latest Jurassic to Early Cretaceous oceanic backarc spreading in the Arperos Basin, separating the Guerrero-Alisitos arc from North America (Cabral-Cano et al., 2000; Centeno-García et al., 2008, 2011; Elias-Herrera et al., 2000; Martini et al., 2011); (4) Early to mid-Cretaceous closure of the Arperos Basin and accretion of the Guerrero and Alisitos arcs to the North American continent, followed by the Late Cretaceous-Eocene Laramide orogeny (Bird, 1988; Coney & Reynolds, 1977; Dickinson et al., 1978; Miller et al., 1992); and (5) Late Eocene to present continental Basin and Range extension (e.g., McQuarrie & Wernicke, 2005; Wernicke, 1981). Hot spot reference frames (e.g., Doubrovine et al., 2012; O'Neill et al., 2005) indicate that North America has been undergoing absolute westward plate motion throughout the Late Cretaceous and Cenozoic. However, earlier absolute plate motions, as well as relative North America-Farallon (or other eastern Panthalassa plates) motions are uncertain, and therefore, the amount of subducted lithosphere within each particular slab segment cannot be determined. Therefore, we focus on the timing and style of upper plate deformation only and relate this to slab geometry.

The upper part of the Cocos slab shallowly plunges down toward the base of the upper mantle which it reaches ~800 km east of the trench (Figure 10, lower left panel: *A*), from where it is flat lying for another ~600 km eastward (*B*). This suggests that the youngest episode of subduction was associated with significant rollback, that is, trench-perpendicular motion of the slab bend relative to the mantle. The southern part of the Cocos slab (subducting below Honduras, south of the Motagua fault zone) does not show this subhorizontal segment (Figure 2a). Since ~50 Ma, the northern part of the Central American land bridge, the continental Chortis block, has been displaced relative to the North American Plate by ~1,100 km along the left-lateral Motagua-Cayman North American-Caribbean transform plate boundary (Boschman et al., 2014). During these last 50 Myr, the Caribbean Plate was near stationary relative to the mantle (Doubrovine et al., 2012), suggesting that the Mexican trench has advanced westward over ~1,100 km since 50 Ma. Additionally, part of the rollback has been accommodated by upper plate extension since ~36 Ma, forming the Basin and Range province (McQuarrie & Wernicke, 2005). Moreover, during the final stages of the Laramide orogeny that

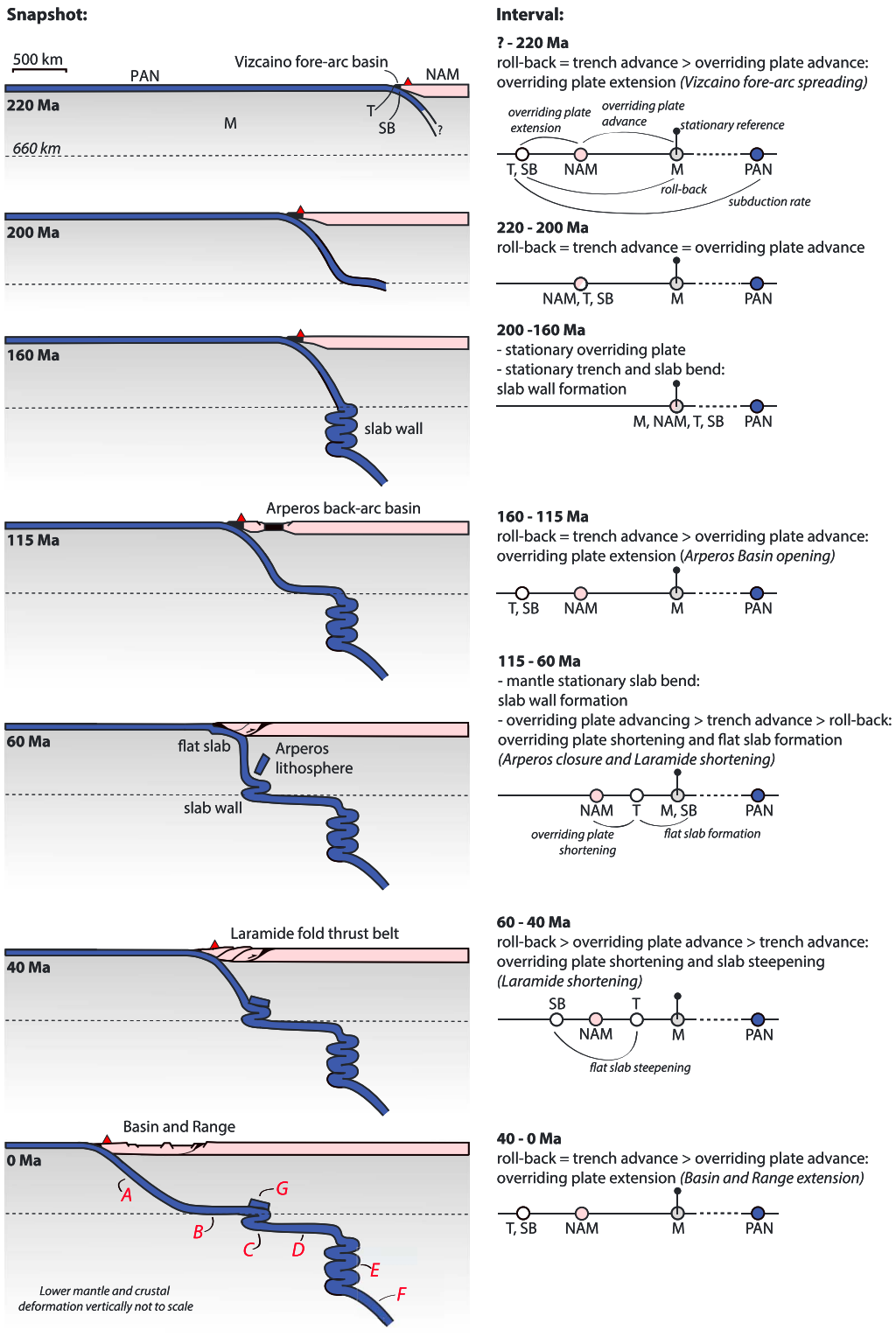

Figure 10. (left column) Cross sections illustrating the step wise evolution of subduction, slab development, and upper plate deformation relative to a stationary mantle. Horizontal and vertical scales are equal, but crustal deformation (vertically exaggerated) and depth of the lower mantle (reduced) are not to scale. (right column) Velocity diagrams per time interval illustrating trench-perpendicular motions of the overriding North American Plate (NAM), the subducting Panthalassa plates (PAN) (Cocos, Farallon, and perhaps additional), the slab bend (SB), and the trench (T), relative to the stationary sublithospheric mantle (M). The trench is the intersection between the subduction thrust and the seafloor; the slab bend the hinge between the horizontal and dipping parts of the subducting plate. Relative motion is represented by a distance on the line (e.g., T left of NAM indicates westward motion of T relative to NAM, and hence, overriding plate extension). Relative motion between SB and T represents flat slab formation or flat slab steepening. The subduction rate is unknown, hence the dashed line between PAN and M.

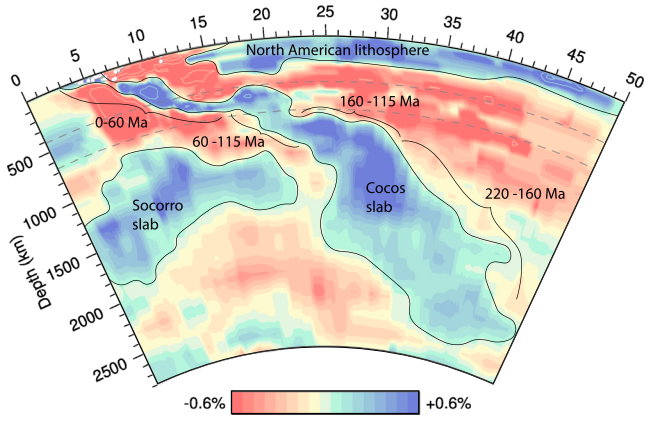

Figure 11. Interpretation of ages of subduction of the shallow-dipping and steep segments of the Cocos slab.

preceded the Basin and Range extensional episode (Figure 10, 60–40 Ma), the flat slab that is widely interpreted to have underlain the western North American margin must have steepened due to rollback, inducing westward motion of the slab bend relative to the trench (T) before overriding plate extension started. We thus interpret the top ~1,400 km of the low-angle to flat slab segment of the Cocos slab to have formed during the waning stages of the Laramide orogeny and throughout the Basin and Range extensional episode, corresponding to subduction evolution during the last ~60 Myr (Figures 10 and 11).

The first small slab wall (*C*) in the mantle transition zone developed due to overriding plate advance and a mantle-stationary slab bend, resulting in closure of the Arperos Basin and subsequent Laramide flat slab formation (115–60 Ma). The slab wall connects to a second (~1,000 km long) flat-lying segment in the top of the lower mantle (*D*), correlated to a phase of rollback exceeding overriding plate advance and upper plate extension, resulting in opening of the Arperos backarc basin (160–115 Ma). During the transition between acceleration (160–115 Ma) and slow down (115–60 Ma) of rollback, relative motion between the slab bend and the overriding plate (NAM) reversed, but formation of the flat lying slab segment D and overriding plate shortening suggests that the North American Plate continuously moved westward relative to the mantle throughout this period (Figure 10).

The major slab wall from ~1,000- to 1,800-km depth in the lower mantle (*E*) suggests an extended period of subduction with a mantle-stationary slab bend leading to the creation of this thickened vertical pile of subducted material. Below ~1,800 km the east dipping anomaly (*F*) has a somewhat thinner appearance than that of the slab wall. This may be an expression of slab stretching following the slab thickening in the slab deceleration zone above ~1,500 km, which results from an increase in sinking velocity below ~1,500 km, presumably related to a decrease in viscosity (van der Meer et al., 2018). We associate this deep eastward dipping portion of the slab down to the lowermost mantle with a period of relatively slow westward slab retreat starting at ~220 Ma. In the period preceding the opening of the Arperos Basin, there is no major overriding plate deformation other than the formation of the Vizcaíno ophiolite. This suggests that North America may have moved up to 1,000 km westward during the Late Triassic (220–200 Ma) and underwent no major longitudinal motion during the Jurassic (200–160 Ma) to create the midmantle slab wall (Figures 10 and 11).

During the Late Triassic to Early Jurassic, the North American Plate underwent absolute northward paleolatitudinal motion according to the TPW-corrected paleomagnetic reference frame (Torsvik et al., 2012; Figure 9), which would suggest that the oldest (Triassic) part of the Mexican record would correlate to a lower mantle slab segment further south in the mantle. We note, however, that while there are large slabs in the lower mantle to the north of the Cocos slab (e.g., the Hatteras slab; van der Meer et al., 2018), there are no slabs to the south that allow for an alternative correlation. We thus tentatively suggest that during the early stages of subduction, when the slab was not yet firmly anchored in the lower mantle, it may have been dragged northward relative to the surrounding and underlying mantle.

No major slab-like anomalies are found to the east of the Cocos slab, indicating that the amount of subducted oceanic lithosphere related to closure of the Arperos Basin was limited. Arperos lithosphere may have merged with the main Cocos slab anomaly, such that it became indistinguishable from subducted Farallon lithosphere (*G*). Paleomagnetic data had already shown that opening and closure of the backarc basin was not associated with significant paleolatitudinal motion (Boschman et al., 2018) and the absence of an identifiable slab now suggests that also paleolongitudinal motions were limited. This indicates that overriding North American plate margin extension or shortening since Triassic time was probably limited to a few hundreds of kilometers during each event. The overall history of absolute paleolongitudinal motion of North America determined here correlates well with the slab-fitted, true polar wander-corrected paleomagnetic reference frame of van der Meer et al. (2010). This frame shows little paleolongitudinal absolute motion of North America between 200 and 150 Ma, both preceded and followed by absolute westward motion.

8.4. Geographical Continuity of the Mesozoic Mexican Subduction System

Currently, subduction of the Cocos Plate continues south of the North American-Caribbean plate boundary. Tectonic reconstructions of the Caribbean region (e.g., Boschman et al., 2014; Pindell & Kennan, 2009), however, show that tectonic terranes with an oceanic basement now forming the Central American land bridge originated in an intra-Panthalassa setting, much further west compared to their present-day location. Eastward subduction at the western Caribbean plate boundary, whereby Farallon lithosphere subducted below the Caribbean Plate, is estimated to have initiated in Santonian (~85 Ma) time, but how or if this trench was connected to the Mexican continental margin trench remains uncertain. Prior to 85 Ma, Farallon-North/South America convergence was taken up by westward subduction of *Proto-Caribbean* lithosphere below the Greater Antilles (e.g., Pindell & Kennan, 2009).

Correlations between the geology of the Vizcaíno-Cedros region and the more northern Californian Franciscan-Coast Range Ophiolite-Great Valley system are striking (Jones et al., 1976; Kimbrough, 1985, 1989; Rangin, 1978; Suppe & Armstrong, 1972). However, in contrast to the Vizcaíno ophiolite, paleomagnetic data from the Coast Range Ophiolite were interpreted to indicate northward motion of the ophiolite relative to North America (Beebe & Luyendyk, 1983; Luyendyk & Hornafius, 1982; McWilliams & Howell, 1982; Williams, 1984). Furthermore, in California, SSZ ophiolites are younger and subduction initiation is interpreted to have occurred in Jurassic time, at ~165 Ma (e.g., Wakabayashi, 2015). This ~55-Myr age difference in along-strike SSZ ophiolites at the western North American margin may be explained in different ways. First, when assuming a shared tectonic history of the ophiolites despite their differences, the age difference may imply that suprasubduction forearc spreading at the Californian margin does not reflect subduction initiation. Recently, Guilmette et al. (2018) showed a 8- to 10-Myr delay between subduction initiation and upper plate extension in the Oman ophiolite, and Maffione and van Hinsbergen (2018) argued that in the Balkan region, the East Vardar SSZ ophiolites may have formed as much as ~70 Myr after subduction initiation. However, Lu/Hf ages of Franciscan metamorphic sole garnets, argued by Guilmette et al. (2018) to record prograde mineral growth during subduction initiation, are ~169 Ma (Anczkiewicz et al., 2004). Alternatively, between ~220 and ~170–165 Ma, the trench north of Vizcaíno may have been offset westward to an intraoceanic setting along a transform fault. Tomographic arguments for such an intraoceanic subduction system were shown in van der Meer et al. (2018), that is, their Socorro slab (Figure 11). This slab is correlated by van der Meer et al. (2018) to Late Triassic to Early Jurassic subduction records of the Wrangellia superterrane that was located at such latitudes at the time (e.g., Enkin, 2006; Johnston, 2001, 2008; Krijgsman & Tauxe, 2006), thereby dividing the Farallon Plate into an eastern plate and a western plate separated by a subduction plate boundary. This intraoceanic subduction system may have temporarily taken up some (but not all) of the convergence at the latitude of the Vizcaíno-Cedros region and further south and may have fully shielded the Californian margin from subduction until the Wrangellia superterrane moved northward toward its present-day location in the Canadian Cordillera and continental margin subduction initiated at ~170–165 Ma. The latter hypothesis explains why uninterrupted subduction resulting in the continuous, exceptionally deep Cocos slab, was restricted to the Mexican part of the Cordillera and why mantle structure further north is considerably more complex. Evidently, even though the vast majority of the Mesozoic eastern Panthalassa Ocean was occupied by the Farallon Plate, differences in interactions with the continental margin of Pangea and the presence of temporal intraoceanic subduction zones resulted in significant regional variations in subduction history.

9. Conclusions

The Vizcaíno-Cedros region of Baja California yields a paleolatitudinal plate motion history equal to that of the North American continent since Late Triassic time. This shows that the Vizcaíno-Cedros region is best interpreted as the forearc of the North American Plate, adjacent to a (>)220-Myr long-lived eastward dipping subduction zone consuming oceanic lithosphere of the eastern Panthalassa Ocean. Tomographic images of the Cocos slab confirm long-lived, uninterrupted eastward subduction. We correlate episodes of overriding plate shortening and extension to steep and flat segments of the slab and provide a first-order, geology, and tomography-constrained tectonic model of the dynamic subduction history of Mexico since the Late Triassic onset of Pangea breakup.

Acknowledgments
We thank Alex Mols for his help in the field and laboratory. L. M. B. acknowledges Netherlands Organization for Scientific Research (NWO) grant 824.01.004; D. J. J. vH acknowledges NWO Vidi grant 864.11.004; W. S. acknowledges support from the Research Council of Norway through its Centres of Excellence funding scheme, project 223272. We thank Nadine McQuarrie for providing the georeferenced files of the Basin and Range reconstruction of McQuarrie and Wernicke (2005), which we used to build the GPlates reconstruction (supporting information Data Set S2). All new and compiled paleomagnetic data (supporting information Data Set S1) can be viewed in the online portal paleomagnetism.org.

References

Alsleben, H., Wetmore, P. H., Gehrels, G., & Paterson, S. (2012). Detrital zircon ages in Palaeozoic and Mesozoic basement assemblages of the Peninsular Ranges batholith, Baja California, Mexico: Constraints for depositional ages and provenance. *International Geology Review*, *54*(1), 93–110.

Amaru, M. (2007). Global travel time tomography with 3-D reference models. (PhD), Utrecht University, (274).

Anczkiewicz, R., Platt, J. P., Thirlwall, M. F., & Wakabayashi, J. (2004). Franciscan subduction off to a slow start: Evidence from high-precision Lu–Hf garnet ages on high grade-blocks. *Earth and Planetary Science Letters*, *225*(1–2), 147–161.

Atwater, T. M. (1998). Late tectonic history of Southern California with emphasis on the Western Transverse ranges and Northern Channel Islands plate tectonic history of Southern California with emphasis on the western Transverse Ranges and Northern Channel Islands.

Barnes, D. A. (1984). Volcanic arc derived, Mesozoic sedimentary rocks, Vizcaino Peninsula, Baja California Sur, Mexico. In V. A. J. Frizzell (Ed.), *Geology of the Baja California Peninsula*, *Pacific Section S.E.P.M.* (Vol. 39, pp. 119–130). Los Angeles, CA: Pacific Section, Society of Economic Paleontologists and Mineralogists (SEPM).

Barnes, D., & Mattison, J. (1981). Late Triassic/Early Cretaceous age of eugeosynclinal terranes, Western Vizcaíno Peninsula, Baja California Sur, México. Geol. *Soc*. *Amer*., *Abstr*. *with Progr*. *Cord*. *Section*, *13*.

Barnes, D. A. (1982). Basin analysis of volcanic arc-derived, Jura-Cretaceous sedimentary rocks, Vizcaìno peninsula, Baja California Sur, Mexico. (PhD), University of California, Santa Barbara.

Barth, A. P., Tosdal, R., Wooden, J., & Howard, K. (1997). Triassic plutonism in southern California: Southward younging of arc initiation along a truncated continental margin. *Tectonics*, *16*, 290–304. https://doi.org/10.1029/96TC03596

Beebe, W., & Luyendyk, B. (1983). Preliminary paleomagnetic results from the Llanada remnant of the Coast Range ophiolite. *San Benito County, California: Eos (Transactions, American Geophysical Union)*, *64*, 686.

Besse, J., & Courtillot, V. (2002). Apparent and true polar wander and the geometry of the geomagnetic field over the last 200 Myr. *Journal of Geophysical Research*, *107*(B11), 2300. https://doi.org/10.1029/2000JB000050

Biggin, A. J., van Hinsbergen, D. J. J., Langereis, C. G., Straathof, G. B., & Deenen, M. H. L. (2008). Geomagnetic secular variation in the Cretaceous Normal Superchron and in the Jurassic. *Physics of the Earth and Planetary Interiors*, *169*(1–4), 3–19.

Bijwaard, H., Spakman, W., & Engdahl, E. R. (1998). Closing the gap between regional and global travel time tomography. *Journal of Geophysical Research*, *103*, 30,055–30,078. https://doi.org/10.1029/98JB02467

Bird, P. (1988). Formation of the Rocky Mountains, western United States: A continuum computer model. *Science*, *239*(4847), 1501–1507.

Boles, J. R., & Landis, C. A. (1984). Jurassic sedimentary mélange and associated facies, Baja California, Mexico. *Geological Society of America Bulletin*, *95*(5).

Boschman, L. M., Garza, R. S. M., Langereis, C. G., & van Hinsbergen, D. J. (2018). Paleomagnetic constraints on the kinematic relationship between the Guerrero terrane (Mexico) and North America since Early Cretaceous time. *GSA Bulletin*, *130*(7–8), 1131–1142.

Boschman, L. M., van Hinsbergen, D. J. J., Torsvik, T. H., Spakman, W., & Pindell, J. L. (2014). Kinematic reconstruction of the Caribbean region since the Early Jurassic. *Earth-Science Reviews*, *138*, 102–136.

Busby, C. J. (2004). Continental growth at convergent margins facing large ocean basins: A case study from Mesozoic convergent-margin basins of Baja California, Mexico. *Tectonophysics*, *392*(1–4), 241–277.

Busby, C. J., Adams, B. F., Mattinson, J., & Deoreo, S. (2006). View of an intact oceanic arc, from surficial to mesozonal levels: Cretaceous Alisitos arc, Baja California. *Journal of Volcanology and Geothermal Research*, *149*(1), 1–46.

Busby, C. J., Smith, D., Morris, W., & Fackler-Adams, B. (1998). Evolutionary model for convergent margins facing large ocean basins: Mesozoic Baja California, Mexico. *Geology*, *26*(3), 227–230.

Busby-Spera, C. J. (1988). Evolution of a Middle Jurassic back-arc basin, Cedros Island, Baja California—Evidence from a marine volcaniclastic apron. *Geological Society of America Bulletin*, *100*(2), 218–233.

Busby-Spera, C. J., & Boles, J. R. (1986). Evolution of subsidence styles in forearc basin: Example from Cretaceous of southern Vizcaino Peninsula, Baja California, Mexico. *American Association of Petroleum Geologists Bulletin*, *70*, 463–464.

Butterworth, N., Talsma, A., Müller, R., Seton, M., Bunge, H.-P., Schuberth, B., et al. (2014). Geological, tomographic, kinematic and geodynamic constraints on the dynamics of sinking slabs. *Journal of Geodynamics*, *73*, 1–13.

Cabral-Cano, E., Lang, H. R., & Harrison, C. G. A. (2000). Stratigraphic assessment of the Arcelia-Teloloapan area, southern Mexico: Implications for southern Mexico's post-Neocomian tectonic evolution. *Journal of South American Earth Sciences*, *13*(4–5), 443–457.

Campa, M. F., & Coney, P. J. (1983). Tectono-stratigraphic terranes and mineral resource distributions in Mexico. *Canadian Journal of Earth Sciences*, *20*(6), 1040–1051.

Centeno-García, E. (2005). Review of Upper Paleozoic and Lower Mesozoic stratigraphy and depositional environments of central and west Mexico: Constraints on terrane analysis and paleogeography. *Geological Society of America Special Papers*, *393*, 233–258.

Centeno-García, E. (2017). Mesozoic tectono-magmatic evolution of Mexico: An overview. *Ore Geology Reviews*, *81*, 1035–1052.

Centeno-García, E., Busby, C., Busby, M., & Gehrels, G. (2011). Evolution of the Guerrero composite terrane along the Mexican margin, from extensional fringing arc to contractional continental arc. *Geological Society of America Bulletin*, *123*(9–10), 1776–1797.

Centeno-García, E., Corona-Chávez, P., Talavera-Mendoza, O., & Iriondo, A. (2003). Geologic and tectonic evolution of the western Guerrero terrane—A transect from Puerto Vallarta to Zihuatanejo, Mexico. Paper presented at the Geologic transects across Cordilleran Mexico, guidebook for the field trips of the 99th Geological Society of America Cordilleran section annual meeting, Puerto Vallarta, Jalisco, Mexico.

Centeno-García, E., Guerrero-Suastegui, M., & Talavera-Mendoza, O. (2008). The Guerrero Composite Terrane of western Mexico: Collision and subsequent rifting in a supra-subduction zone. In *Special Paper 436: Formation and Applications of the Sedimentary Record in Arc Collision Zones* (pp. 279–308).

Centeno-García, E., Ruíz, J., Coney, P. J., Patchett, P. J., & Ortega-Gutiérrez, F. (1993). Guerrero terrane of Mexico: Its role in the Southern, Cordillera from new geochemical data. *Geology*, *21*(5), 419–422.

Coney, P. J., & Reynolds, S. J. (1977). Cordilleran benioff zones. *Nature*, *270*(5636), 403.

Critelli, S., Marsaglia, K. M., & Busby, C. J. (2002). Tectonic history of a Jurassic backarc-basin sequence (the Gran Cañon Formation, Cedros Island, Mexico), based on compositional modes of tuffaceous deposits. *Geological Society of America Bulletin*, *114*(5), 515–527.

Debiche, M. G., Cox, A., & Engebretson, D. C. (1987). *The motion of allochthonous terranes across the North Pacific basin*. Boulder, CO: Geological Society of America.

Deenen, M. H. L., Langereis, C. G., van Hinsbergen, D. J. J., & Biggin, A. J. (2011). Geomagnetic secular variation and the statistics of palaeomagnetic directions. *Geophysical Journal International*, *186*(2), 509–520.

DePaolo, D. J. (1981). A neodymium and strontium isotopic study of the Mesozoic calc-alkaline granitic batholiths of the Sierra Nevada and Peninsular Ranges, California. *Journal of Geophysical Research*, *86*, 10,470–10,488. https://doi.org/10.1029/Jb086ib11p10470

Dickinson, W. R., Snyder, W. S., & Matthews, V. (1978). Plate tectonics of the Laramide orogeny (Vol. 3): Matthews.
Dilek, Y., & Furnes, H. (2011). Ophiolite genesis and global tectonics: Geochemical and tectonic fingerprinting of ancient oceanic lithosphere. *Bulletin*, *123*(3–4), 387–411.
Domeier, M., Shephard, G. E., Jakob, J., Gaina, C., Doubrovine, P. V., & Torsvik, T. H. (2017). Intraoceanic subduction spanned the Pacific in the Late Cretaceous–Paleocene. *Science Advances*, *3*(11), eaao2303.
Doubrovine, P. V., Steinberger, B., & Torsvik, T. H. (2012). Absolute plate motions in a reference frame defined by moving hot spots in the Pacific, Atlantic, and Indian oceans. *Journal of Geophysical Research*, *117*, B09101. https://doi.org/10.1029/2011JB009072
Elders, W. A., Rex, R. W., Robinson, P. T., Biehler, S., & Meidav, T. (1972). Crustal spreading in Southern California: The Imperial Valley and the Gulf of California formed by the rifting apart of a continental plate. *Science*, *178*(4056), 15–24.
Elias-Herrera, M., Sanchez-Zavala, J. L., & Macias-Romo, C. (2000). Geologic and geochronologic data from the Guerrero terrane in the Tejupilco area, southern Mexico: New constraints on its tectonic interpretation. *Journal of South American Earth Sciences*, *13*(4–5), 355–375.
Engebretson, D. C., Cox, A., & Gordon, R. G. (1985). Relative motions between oceanic and continental plates in the Pacific Basin. *Geological Society of America Special Papers*, *206*. https://doi.org/10.1130/SPE206-p1
Enkin, R. J. (2006). Paleomagnetism and the case for Baja British Columbia. In J. W. Haggart, R. J. Enkin, & J. W. H. Monger (Eds.), *Paleogeography of the North American Cordillera: Evidence for and against large-scale displacements*, *Special Paper* (Vol. 46, pp. 233–253). St. John's: Geological Association of Canada.
Faccenna, C., Funiciello, F., Giardini, D., & Lucente, P. (2001). Episodic back-arc extension during restricted mantle convection in the Central Mediterranean. *Earth and Planetary Science Letters*, *187*(1–2), 105–116.
Faccenna, C., Piromallo, C., Crespo-Blanc, A., Jolivet, L., & Rossetti, F. (2004). Lateral slab deformation and the origin of the western Mediterranean arcs. *Tectonics*, *23*, TC1012. https://doi.org/10.1029/2002TC00148
Ferrari, L., Valencia-Moreno, M., & Bryan, S. (2007). Magmatism and tectonics of the Sierra Madre Occidental and its relation with the evolution of the western margin of North America. In Special Paper 422: Geology of México: Celebrating the Centenary of the Geological Society of México (pp. 1–39).
Finch, J. W., & Abbott, P. L. (1977). Petrology of a Triassic Marine Section, Vizcaino Peninsula, Baja California Sur, Mexico. *Sedimentary Geology*, *19*(4), 253–273.
Fisher, R. (1953). Dispersion on a sphere. *Proceedings of the Royal Society A: Mathematical, Physical and Engineering Sciences*, *217*(1130), 295–305.
Funiciello, F., Faccenna, C., & Giardini, D. (2004). Role of lateral mantle flow in the evolution of subduction systems: Insights from laboratory experiments. *Geophysical Journal International*, *157*(3), 1393–1406.
Gastil, R. G., Phillips, R. P., & Allison, E. C. (1975). Reconnaissance geology of the state of Baja California. *Geological Society of America Memoirs*, *140*, 1–201.
Gradstein, F. M., Ogg, J. G., Schmitz, M., & Ogg, G. (2012). *The geologic time scale 2012*. Amsterdam: Elsevier.
Grand, S. P., van der Hilst, R. D., & Widiyantoro, S. (1997). Global seismic tomography: A snapshot of convection in the Earth. *GSA Today*, *7*(4), 1–7.
Gromet, P., & Silver, L. T. (1987). REE variations across the Peninsular Ranges batholith: Implications for batholithic petrogenesis and crustal growth in magmatic arcs. *Journal of Petrology*, *28*(1), 75–125.
Guilmette, C., Smit, M. A., van Hinsbergen, D. J., Gürer, D., Corfu, F., Charette, B., et al. (2018). Forced subduction initiation recorded in the sole and crust of the Semail Ophiolite of Oman. *Nature Geoscience*, *1*.
Gürer, D., Hinsbergen, D. J., Matenco, L., Corfu, F., & Cascella, A. (2016). Kinematics of a former oceanic plate of the Neotethys revealed by deformation in the Ulukışla basin (Turkey). *Tectonics*, *35*, 2385–2416. https://doi.org/10.1002/2016TC004206
Hafkenscheid, E., Wortel, M., & Spakman, W. (2006). Subduction history of the Tethyan region derived from seismic tomography and tectonic reconstructions. *Journal of Geophysical Research*, *111*, B08401. https://doi.org/10.1029/2005JB003791
Hagstrum, J. T., Martínez, M. L., & York, D. (1993). Paleomagnetic and 40Ar/39Ar evidence for remagnetization of Mesozoic oceanic rocks on the Vizcaino Peninsula, Baja California Sur, Mexico. *Geophysical Research Letters*, *20*, 1831–1834. https://doi.org/10.1029/93GL02010
Hagstrum, J. T., McWillams, M., Howell, D. G., & Grommé, S. (1985). Mesozoic paleomagnetism and northward translation of the Baja California Peninsula. *Geological Society of America Bulletin*, *96*, 1077–1090.
Hall, R., & Spakman, W. (2002). Subducted slabs beneath the eastern Indonesia–Tonga region: Insights from tomography. *Earth and Planetary Science Letters*, *201*(2), 321–336.
Heuret, A., & Lallemand, S. (2005). Plate motions, slab dynamics and back-arc deformation. *Physics of the Earth and Planetary Interiors*, *149*(1–2), 31–51.
Hickey, J. J. (1984). Stratigraphy and composition of a Jura-Cretaceous volcanic arc apron, Punta Eugenia, Baja California Sur, Mexico. In V. A. J. Frizzell (Ed.), *Geology of the Baja California peninsula*, *Field Trip Guidebook, Pacific Section: Society of Economic Paleontologists and Miner- alogists Pacific Section* (Vol. 39, pp. 149–160). Los Angeles, CA: Pacific Section, Society of Economic Paleontologists and Mineralogists (SEPM).
Hildebrand, R. S. (2013). *Mesozoic assembly of the North American Cordillera*, *Special Paper* (Vol. 495). Boulder, Colo.: The Geological Society of America.
Huang, W., Van Hinsbergen, D. J., Maffione, M., Orme, D. A., Dupont-Nivet, G., Guilmette, C., et al. (2015). Lower Cretaceous Xigaze ophiolites formed in the Gangdese forearc: Evidence from paleomagnetism, sediment provenance, and stratigraphy. *Earth and Planetary Science Letters*, *415*, 142–153.
Johnson, C. L., Constable, C. G., Tauxe, L., Barendregt, R., Brown, L. L., Coe, R. S., et al. (2008). Recent investigations of the 0-5 Ma geomagnetic field recorded by lava flows. *Geochemistry, Geophysics, Geosystems*, *9*, Q04032. https://doi.org/10.1029/2007GC001696
Johnson, S. E., Tate, M. C., & Mark Fanning, C. (1999). New geologic mapping and SHRIMP U-Pb zircon data in the Peninsular Ranges batholith, Baja California, Mexico: Evidence for a suture? *Geology*, *27*(8).
Johnston, S. T. (2001). The Great Alaskan Terrane Wreck: reconciliation of paleomagnetic and geological data in the northern Cordillera. *Earth and Planetary Science Letters*, *193*(3–4), 259–272.
Johnston, S. T. (2008). The cordilleran ribbon continent of North America. *Annual Review of Earth and Planetary Sciences*, *36*, 495–530.
Jones, D. L., Blake, M. Jr., & Rangin, C. (1976). The four Jurassic belts of northern California and their significance to the geology of the southern California borderland. In D. G. Howell (Ed.), *Aspects of the geologic history of the California continental borderland*, *Vol. Pacific section miscellaneous publication* (Vol. 24, pp. 343–362). Tulsa, OK: American Association of Petroleum Geologists.
Jordan, T. H., & Lynn, W. S. (1974). A velocity anomaly in the lower mantle. *Journal of Geophysical Research*, *79*, 2679–2685. https://doi.org/10.1029/JB079i017p02679
Kent, D. V., & Irving, E. (2010). Influence of inclination error in sedimentary rocks on the Triassic and Jurassic apparent pole wander path for North America and implications for Cordilleran tectonics. *Journal of Geophysical Research*, *115*, B10103. https://doi.org/10.1029/2009JB007205

Kimbrough, D. L. (1985). Tectonostratigraphic Terranes of the Vizcaino Peninsula and Cedros and San Benito Islands, Baja California, Mexico. In *Tectonostratigrahic terranes of the circum-Pacific region*, *Vol. Earth Science Series* (pp. 285–298). American Association of Petroleum Geologists.

Kimbrough, D. L. (1989). *Franciscan complex rocks on Cedros Island*. Baja California Sur, Mexico: Radiolarian biostratigraphic ages from a chert mélange block and petrographic observations on metasandstone.

Kimbrough, D. L., Abbott, P. L., Balch, D. C., Bartling, S. H., Grove, M., Mahoney, J. B., & Donohue, R. F. (2014). Upper Jurassic Peñasquitos Formation—Forearc basin western wall rock of the Peninsular Ranges batholith. In *Peninsular ranges Batholith, Baja California and Southern California* (pp. 625–643). Geological Society of America Memoirs.

Kimbrough, D. L., Abbott, P. L., Grove, M., Smith, D. P., Mahoney, J. B., Moore, T. E., & Gehrels, G. (2006). Contrasting cratonal provinces for Upper Cretaceous Valle Group quartzite lasts, Baja California. In Using Stratigraphy, Sedimentology, and Geochemistry to Unravel the Geologic History of the Southwestern Cordillera: A Volume in Honor of Patrick L. Abbott (pp. 97–110). Los Angeles, CA: Pacific Section, Society of Economic Paleontologists and Mineralogists (SEPM).

Kimbrough, D. L., & Moore, T. E. (2003). Ophiolite and volcanic arc assemblages on the Vizcaino Peninsula and Cedros Island, Baja California Sur, Mexico: Mesozoic for ear c lithosphere of the Cordilleran magmatic arc. *Tectonic evolution of northwestern Mexico and the southwestern USA*, *374*, 43.

Kimbrough, D. L., Smith, D. P., Mahoney, J. B., Moore, T. E., Grove, M., Gastil, R. G., et al. (2001). Forearc-basin sedimentary response to rapid Late Cretaceous batholith emplacement in the Peninsular Ranges of southern and Baja California. *Geology*, *29*(6), 491–494.

Kirschvink, J. L. (1980). The least-squares line and plane and the analysis of palaeomagnetic data. *Geophysical Journal International*, *62*, 699–718.

Koymans, M. R., Langereis, C. G., Pastor-Galán, D., & van Hinsbergen, D. J. J. (2016). Paleomagnetism.org: An online multi-platform open source environment for paleomagnetic data analysis. *Computers & Geosciences*, *93*, 127–137.

Krijgsman, W., & Tauxe, L. (2006). E/I corrected paleolatitudes for the sedimentary rocks of the Baja British Columbia hypothesis. *Earth and Planetary Science Letters*, *242*(1–2), 205–216.

Lallemand, S., Heuret, A., & Boutelier, D. (2005). On the relationships between slab dip, back-arc stress, upper plate absolute motion, and crustal nature in subduction zones. *Geochemistry, Geophysics, Geosystems*, *6*, Q09006. https://doi.org/10.1029/2005GC000917

Larson, R. L., Menard, H., & Smith, S. (1968). Gulf of California: A result of ocean-floor spreading and transform faulting. *Science*, *161*(3843), 781–784.

Li, S., Advokaat, E. L., van Hinsbergen, D. J., Koymans, M., Deng, C., & Zhu, R. (2017). Paleomagnetic constraints on the Mesozoic-Cenozoic paleolatitudinal and rotational history of Indochina and South China: Review and updated kinematic reconstruction. *Earth-Science Reviews*, *171*, 58–77.

Liu, L. (2014). Constraining Cretaceous subduction polarity in eastern Pacific from seismic tomography and geodynamic modeling. *Geophysical Research Letters*, *41*, 8029–8036. https://doi.org/10.1002/2014GL061988

Liu, L., Gurnis, M., Seton, M., Saleeby, J., Müller, R. D., & Jackson, J. M. (2010). The role of oceanic plateau subduction in the Laramide orogeny. *Nature Geoscience*, *3*(5), 353–357.

Lonsdale, P. (1989). Geology and tectonic history of the Gulf of California. In *The eastern Pacific Ocean and Hawaii* (pp. 499–521). Boulder, Colorado: Geological Society of America, Geology of North America, v. N.

Lonsdale, P., Blum, N., & Puchelt, H. (1992). The Rrr triple junction at the southern end of the Pacific-Cocos East Pacific Rise. *Earth and Planetary Science Letters*, *109*(1–2), 73–85.

Luyendyk, B., & Hornafius, J. (1982). Paleolatitude of the Point Sal ophiolite. Paper presented at the Geological Society of America Abstracts with Programs.

Maffione, M., Hinsbergen, D. J., Gelder, G. I., Goes, F. C., & Morris, A. (2017). Kinematics of Late Cretaceous subduction initiation in the Neo-Tethys Ocean reconstructed from ophiolites of Turkey, Cyprus, and Syria. *Journal of Geophysical Research: Solid Earth*, *122*, 3953–3976. https://doi.org/10.1002/2016JB013821

Maffione, M., Thieulot, C., van Hinsbergen, D. J. J., Morris, A., Plümper, O., & Spakman, W. (2015). Dynamics of intraoceanic subduction initiation: 1. Oceanic detachment fault inversion and the formation of supra-subduction zone ophiolites. *Geochemistry, Geophysics, Geosystems*, *16*, 1753–1770. https://doi.org/10.1002/2015GC005746

Maffione, M., & van Hinsbergen, D. J. (2018). Reconstructing plate boundaries in the Jurassic Neo-Tethys from the East and West Vardar ophiolites (Greece and Serbia). *Tectonics*, *37*, 858–887. https://doi.org/10.1002/2017TC004790

Maffione, M., Van Hinsbergen, D. J., Koornneef, L. M., Guilmette, C., Hodges, K., Borneman, N., et al. (2015). Forearc hyperextension dismembered the south Tibetan ophiolites. *Geology*, *43*(6), 475–478.

Martini, M., Mori, L., Solari, L., & Centeno-García, E. (2011). Sandstone provenance of the Arperos Basin (Sierra de Guanajuato, Central Mexico): Late Jurassic–Early Cretaceous back-arc spreading as the foundation of the Guerrero Terrane. *The Journal of Geology*, *119*(6), 597–617.

McQuarrie, N., & Wernicke, B. P. (2005). An animated tectonic reconstruction of southwestern North America since 36 Ma. *Geosphere*, *1*(3), 147–172.

McWilliams, M., & Howell, D. (1982). Exotic terranes of western California. *Nature*, *297*(5863), 215–217.

Metcalf, R. V., & Shervais, J. W. (2008). Suprasubduction-zone ophiolites: Is there really an ophiolite conundrum? *Geological Society of America Special Papers*, *438*, 191–222.

Miller, D., Nilsen, T., & Bilodeau, W. (1992). Late Cretaceous to early Eocene geologic evolution of the US Cordillera. *The Geology of North America*, *3*, 205–260.

Miller, M. S., Gorbatov, A., & Kennett, B. (2005). Heterogeneity within the subducting Pacific slab beneath the Izu–Bonin–Mariana arc: Evidence from tomography using 3D ray tracing inversion techniques. *Earth and Planetary Science Letters*, *235*(1–2), 331–342.

Minch, J. C., Gastil, G., Fink, W., Robinson, J., & James, A. H. (1976). Geology of the Vizcaino Peninsula.

Moix, P., Beccaletto, L., Kozur, H. W., Hochard, C., Rosselet, F., & Stampfli, G. M. (2008). A new classification of the Turkish terranes and sutures and its implication for the paleotectonic history of the region. *Tectonophysics*, *451*(1), 7–39.

Moore, T. E. (1983). Geology, petrology, and tectonic significance of the Mesozoic paleooceanic terranes of the Vizcaíno peninsula, Baja California Sur, Mexico. (PhD), Stanford University, Stanford, California.

Moore, T. E. (1984). Sedimentary facies and composition of Jurassic volcaniclastic turbidites at Cerro El Calvario, Vizcaino Peninsula, Baja California Sur, Mexico. In V. A. J. Frizzell (Ed.), *Geology of the Baja California Peninsula*, *Pacifc Section S.E.P.M* (Vol. 39, pp. 131–147). Los Angeles, CA: Pacific Section, Society of Economic Paleontologists and Mineralogists (SEPM).

Moore, T. E. (1985). Stratigraphic and tectonic significance of the Mesozoic tectonostratigraphic terranes of the Vizcaíno peninsula, Baja California Sur, Mexico. In D. G. Howell (Ed.), *Tectonostratigraphic terranes of the circum-Pacific region* (pp. 315–329). Houston, Texas: Circum-Pacific Council for Energy and Mineral Resources.

Moore, T. E. (1986). Petrology and tectonic implications of the blueschist-bearing Puerto Nuevo melange complex, Vizcaino Peninsula, Baja California Sur, Mexico. *Geological Society of America Memoirs*, *164*, 43–58.

Mullender, T. A., Frederichs, T., Hilgenfeldt, C., de Groot, L. V., Fabian, K., & Dekkers, M. J. (2016). Automated paleomagnetic and rock magnetic data acquisition with an in-line horizontal "2G" system. *Geochemistry, Geophysics, Geosystems*, *17*, 3546–3559. https://doi.org/10.1002/2016GC006436

Mullender, T. A. T., Vanvelzen, A. J., & Dekkers, M. J. (1993). Continuous Drift Correction and Separate Identification of Ferrimagnetic and Paramagnetic Contributions in Thermomagnetic Runs. *Geophysical Journal International*, *114*(3), 663–672.

Nokleberg, W. J. (2000). *Phanerozoic tectonic evolution of the circum-North Pacific*. Denver: U.S. Dept. of the Interior, U.S. Geological Survey.

Obrebski, M., Allen, R. M., Xue, M., & Hung, S. H. (2010). Slab-plume interaction beneath the Pacific Northwest. *Geophysical Research Letters*, *37*, L14305. https://doi.org/10.1029/2010GL043489.

O'Neill, C., Müller, D., & Steinberger, B. (2005). On the uncertainties in hot spot reconstructions and the significance of moving hot spot reference frames. *Geochemistry, Geophysics, Geosystems*, *6*, Q04003. https://doi.org/10.1029/2004GC000784

Ortega-Flores, B., Solari, L., Lawton, T. F., & Ortega-Obregón, C. (2014). Detrital-zircon record of major Middle Triassic–Early Cretaceous provenance shift, central Mexico: Demise of Gondwanan continental fluvial systems and onset of back-arc volcanism and sedimentation. *International Geology Review*, *56*(2), 237–261.

Patterson, D. L. (1984). Paleomagnetism of the Valle Formation and the Late Cretaceous paleogeography of the Vizcaino Basin, Baja California, Mexico. In V. A. J. Frizzell (Ed.), *Geology of the Baja California Peninsula*, *Vol. Pacific Section S.E.P.M* (Vol. 39, pp. 173–182). Los Angeles, CA: Pacific Section, Society of Economic Paleontologists and Mineralogists (SEPM).

Pessagno, E. A., Finch, W., & Abbott, P. L. (1979). Upper Triassic Radiolaria from the San Hipolito Formation, Baja California. *Micropaleontology*, *25*, 160–197.

Pindell, J. L., & Kennan, L. (2009). Tectonic evolution of the Gulf of Mexico, Caribbean and northern South America in the mantle reference frame: An update. *Geological Society, London, Special Publications*, *328*(1), 1.1–1.55.

Pozzi, J., Westphal, M., Girardeau, J., Besse, J., Zhou, Y. X., Chen, X. Y., & Xing, L. S. (1984). Paleomagnetism of the Xigaze ophiolite and flysch (Yarlung Zangbo suture zone, southern Tibet): Latitude and direction of spreading. *Earth and Planetary Science Letters*, *70*(2), 383–394.

Premo, W. R., Morton, D. M., Wooden, J. L., & Fanning, C. M. (2014). U-Pb zircon geochronology of plutonism in the northern Peninsular Ranges batholith, southern California: Implications for the Late Cretaceous tectonic evolution of southern California. In *Peninsular Ranges Batholith, Baja California and Southern California* (pp. 145–180). Geological Society of America Memoirs.

Rangin, C. (1978). Speculative model of Mesozoic geodynamics, central Baja California to northeastern Sonora (Mexico). In *Mesozoic paleogeography of the Western United States*, *Pacific Section S.E.P.M* (pp. 85–106). Los Angeles, CA: Pacific Section, Society of Economic Paleontologists and Mineralogists (SEPM).

Rangin, C., Girard, D., & Maury, R. (1983). Geodynamic significance of Late Triassic to Early Cretaceous volcanic sequences of Vizcaino Peninsula and Cedlros Island, Baja California, Mexico. *Geology*, *11*, 552–556.

Rawlinson, N., & Spakman, W. (2016). On the use of sensitivity tests in seismic tomography. *Geophysical Journal International*, *205*(2), 1221–1243.

Saleeby, J. (1981). Ocean floor accretion and volcanoplutonic arc evolution of the Mesozoic Sierra Nevada. In: *The geotectonic development of California*. Rubey volume No. 1, Prentice-Hall, Englewood, 132–181.

Saleeby, J. (1992). Petrotectonic and paleogeographic settings of US Cordilleran ophiolites. In *The Cordilleran Orogen: Conterminous US* (pp. 653–682). Boulder, Colorado: the Geology of North America.

Schellart, W. P. (2008a). Overriding plate shortening and extension above subduction zones: A parametric study to explain formation of the Andes Mountains. *Geological Society of America Bulletin*, *120*(11–12), 1441–1454.

Schellart, W. P. (2008b). Subduction zone trench migration: Slab driven or overriding-plate-driven? *Physics of the Earth and Planetary Interiors*, *170*(1–2), 73–88.

Schepers, G., van Hinsbergen, D. J. J., Spakman, W., Kosters, M. E., Boschman, L. M., & McQuarrie, N. (2017). South-American plate advance and forced Andean trench retreat as drivers for transient flat subduction episodes. *Nature Communications*, *8*, 15249. https://www.ncbi.nlm.nih.gov/pubmed/28508893

Schmidt, K. L., Wetmore, P. H., Alsleben, H., & Paterson, S. R. (2014). Mesozoic tectonic evolution of the southern Peninsular Ranges batholith, Baja California, Mexico: Long-lived history of a collisional segment in the Mesozoic Cordilleran arc. In *Peninsular ranges batholith, Baja California and Southern California* (pp. 645–668). Geological Society of America Memoirs.

Schmidt, K. L., Wetmore, P. H., Johnson, S., & Paterson, S. (2002). Controls on orogenesis along an ocean-continent margin transition in the Jura-Cretaceous Peninsular Ranges batholith. *Geological Society of America Special Papers*, *365*, 49–72.

Shephard, G. E., Matthews, K. J., Hosseini, K., & Domeier, M. (2017). On the consistency of seismically imaged lower mantle slabs. *Scientific Reports*, *7*(1), 10976.

Shephard, G. E., Müller, R. D., & Seton, M. (2013). The tectonic evolution of the Arctic since Pangea breakup: Integrating constraints from surface geology and geophysics with mantle structure. *Earth-Science Reviews*, *124*, 148–183.

Shervais, J. W., Kimbrough, D. L., Renne, P., Hanan, B. B., Murchey, B., Snow, C. A., et al. (2004). Multi-stage origin of the coast range ophiolite, California: Implications for the life cycle of supra-subduction zone ophiolites. *International Geology Review*, *46*(4), 289–315.

Sigloch, K., & Mihalynuk, M. G. (2013). Intra-oceanic subduction shaped the assembly of Cordilleran North America. *Nature*, *496*(7443), 50–56. https://www.ncbi.nlm.nih.gov/pubmed/23552944

Sigloch, K., & Mihalynuk, M. G. (2017). Mantle and geological evidence for a Late Jurassic–Cretaceous suture spanning North America. *GSA Bulletin*, *129*(11–12), 1489–1520.

Silver, L., & Chappell, B. (1988). The peninsular ranges batholith: An insight into the evolution of the Cordilleran batholiths of southwestern North America. *Earth and Environmental Science Transactions of the Royal Society of Edinburgh*, *79*(2–3), 105–121.

Silver, L., Taylor, H., & Chappell, B. (1979). Some petrological, geochemical and geochronological observations of the Peninsular Ranges batholith near the international border of the USA and Mexico. Paper presented at the Mesozoic Crystalline Rocks: Geological Society of America, Annual Meeting, Guidebook.

Smith, D. P., & Busby, C. J. (1993). Shallow magnetic inclinations in the Cretaceous Valle Group, Baja California: Remagnetization, compaction, or terrane translation? *Tectonics*, *12*, 1258–1266. https://doi.org/10.1029/93TC01378

Spakman, W., Chertova, M. V., van den Berg, A., & van Hinsbergen, D. J. (2018). Puzzling features of western Mediterranean tectonics explained by slab dragging. *Nature Geoscience*, *11*(3), 211.

Spakman, W., & Hall, R. (2010). Surface deformation and slab–mantle interaction during Banda arc subduction rollback. *Nature Geoscience*, *3*(8), 562.

Spakman, W., & Wortel, R. (2004). A tomographic view on western Mediterranean geodynamics. In *The TRANSMED Atlas. The Mediterranean region from crust to mantle* (pp. 31–52). Berlin: Springer.

Steinberger, B., & Torsvik, T. H. (2008). Absolute plate motions and true polar wander in the absence of hotspot tracks. *Nature*, *452*(7187), 620–623. https://www.ncbi.nlm.nih.gov/pubmed/18385737

Stern, R. J., & Bloomer, S. H. (1992). Subduction zone infancy—Examples from the Eocene Izu-Bonin-Mariana and Jurassic California Arcs. *Geological Society of America Bulletin*, *104*(12), 1621–1636.
Stern, R. J., Reagan, M., Ishizuka, O., Ohara, Y., & Whattam, S. (2012). To understand subduction initiation, study forearc crust: To understand forearc crust, study ophiolites. *Lithosphere*, *4*(6), 469–483.
Stock, J. M., & Hodges, K. V. (1989). Pre-Pliocene extension around the Gulf of California and the transfer of Baja California to the Pacific Plate. *Tectonics*, *8*, 99–115. https://doi.org/10.1029/TC008i001p00099
Suppe, J., & Armstrong, R. L. (1972). Potassium-argon dating of Franciscan metamorphic rocks. *American Journal of Science*, *272*(3), 217–233.
Talavera-Mendoza, O., Ruiz, J., Gehrels, G. E., Valencia, V. A., & Centeno-Garcia, E. (2007). Detrital zircon U/Pb geochronology of southern Guerrero and western Mixteca arc successions (southern Mexico): New insights for the tectonic evolution of southwestern North America during the late Mesozoic. *Geological Society of America Bulletin*, *119*(9–10), 1052–1065.
Tauxe, L. (2010). *Essentials of paleomagnetism*. Berkeley: Univ of California Press.
Tauxe, L., & Kent, D. V. (2004). A simplified statistical model for the geomagnetic field and the detection of shallow bias in paleomagnetic inclinations: Was the ancient magnetic field dipolar? *Timescales of the Paleomagnetic field*, 101–115. https://doi.org/10.1029/145GM08
Tauxe, L., & Watson, G. S. (1994). The Fold Test - an Eigen Analysis Approach. *Earth and Planetary Science Letters*, *122*(3–4), 331–341.
Todd, V., & Shaw, S. (1985). S-type granitoids and an IS line in the Peninsular Ranges batholith, southern California. *Geology*, *13*(4), 231–233.
Topuz, G., Çelık, Ö. F., Şengör, A. C., Altintaş, İ. E., Zack, T., Rolland, Y., & Barth, M. (2013). Jurassic ophiolite formation and emplacement as backstop to a subduction-accretion complex in northeast Turkey, the Refahıye ophiolite, and relation to the Balkan ophiolites. *American Journal of Science*, *313*(10), 1054–1087.
Topuz, G., Göçmengil, G., Rolland, Y., Çelik, Ö. F., Zack, T., & Schmitt, A. K. (2013). Jurassic accretionary complex and ophiolite from northeast Turkey: No evidence for the Cimmerian continental ribbon. *Geology*, *41*(2), 255–258.
Torres-Carrillo, X. G., Delgado-Argote, L. A., Böhnel, H., Molina-Garza, R. S., & Weber, B. (2016). Palaeomagnetic assessment of plutons from the southern Peninsular Ranges batholith and the Jurassic Vizcaíno igneous suites, Baja California, México. *International Geology Review*, *58*(4), 489–509.
Torsvik, T. H., & Cocks, L. R. M. (2016). *Earth history and palaeogeography*. Cambridge: Cambridge University Press.
Torsvik, T. H., van der Voo, R., Doubrovine, P. V., Burke, K., Steinberger, B., Ashwal, L. D., et al. (2014). Deep mantle structure as a reference frame for movements in and on the Earth. *Proceedings of the National Academy of Sciences of the United States of America*, *111*(24), 8735–8740. https://www.ncbi.nlm.nih.gov/pubmed/24889632
Torsvik, T. H., Van der Voo, R., Preeden, U., Mac Niocaill, C., Steinberger, B., Doubrovine, P. V., et al. (2012). Phanerozoic polar wander, palaeogeography and dynamics. *Earth-Science Reviews*, *114*(3–4), 325–368.
Troughton, G. H. (1974). Stratigraphy of the Vizcaíno Peninsula near Asunción Bay, Territorio de Baja California, Mexico. (MSc).
Van de Lagemaat, S. H. A., van Hinsbergen, D. J. J., Boschman, L. M., Kamp, P. J. J., & Spakman, W. (2018). Southwest Pacific absolute plate kinematic reconstruction reveals major mid- to Late Cenozoic Tonga-Kermadec slab dragging. *Tectonics*, *37*. https://doi.org/10.1029/2017TC004901
van der Hilst, R., & Seno, T. (1993). Effects of relative plate motion on the deep structure and penetration depth of slabs below the Izu-Bonin and Mariana island arcs. *Earth and Planetary Science Letters*, *120*(3–4), 395–407.
van der Hilst, R. D. (1995). Complex morphology of subducted lithosphere in the mantle beneath the Tonga trench. *Nature*, *374*(6518), 154.
van der Meer, D. G., Spakman, W., van Hinsbergen, D. J. J., Amaru, M. L., & Torsvik, T. H. (2010). Towards absolute plate motions constrained by lower-mantle slab remnants. *Nature Geoscience*, *3*(1), 36–40.
van der Meer, D. G., Torsvik, T. H., Spakman, W., van Hinsbergen, D. J. J., & Amaru, M. L. (2012). Intra-Panthalassa Ocean subduction zones revealed by fossil arcs and mantle structure. *Nature Geoscience*, *5*(3), 215–219.
van der Meer, D. G., van Hinsbergen, D. J., & Spakman, W. (2018). Atlas of the underworld: Slab remnants in the mantle, their sinking history, and a new outlook on lower mantle viscosity. *Tectonophysics*, *723*, 309–448.
Van der Voo, R., Spakman, W., & Bijwaard, H. (1999a). Mesozoic subducted slabs under Siberia. *Nature*, *397*(6716), 246.
Van der Voo, R., Spakman, W., & Bijwaard, H. (1999b). Tethyan subducted slabs under India. *Earth and Planetary Science Letters*, *171*(1), 7–20.
van Hinsbergen, D. J. J., de Groot, L. V., van Schaik, S. J., Spakman, W., Bijl, P. K., Sluijs, A., et al. (2015). A paleolatitude calculator for paleoclimate studies. *PLoS One*, *10*(6), e0126946. https://www.ncbi.nlm.nih.gov/pubmed/26061262
van Hinsbergen, D. J. J., Hafkenscheid, E., Spakman, W., Meulenkamp, J. E., & Wortel, R. (2005). Nappe stacking resulting from subduction of oceanic and continental lithosphere below Greece. *Geology*, *33*(4), 325.
van Hinsbergen, D. J. J., Peters, K., Maffione, M., Spakman, W., Guilmette, C., Thieulot, C., et al. (2015). Dynamics of intraoceanic subduction initiation: 2. Suprasubduction zone ophiolite formation and metamorphic sole exhumation in context of absolute plate motions. *Geochemistry, Geophysics, Geosystems*, *16*, 1771–1785. https://doi.org/10.1002/2015GC005745
Vaughn, J., Kodama, K. P., & Smith, D. P. (2005). Correction of inclination shallowing and its tectonic implications: The cretaceous Perforada Formation, Baja California. *Earth and Planetary Science Letters*, *232*(1–2), 71–82.
Wakabayashi, J. (2015). Anatomy of a subduction complex: Architecture of the Franciscan Complex, California, at multiple length and time scales. *International Geology Review*, *57*(5–8), 669–746.
Wakabayashi, J., Ghatak, A., & Basu, A. R. (2010). Suprasubduction-zone ophiolite generation, emplacement, and initiation of subduction: A perspective from geochemistry, metamorphism, geochronology, and regional geology. *Geological Society of America Bulletin*, *122*(9–10), 1548–1568.
Wernicke, B. (1981). Low-angle normal faults in the Basin and Range Province: Nappe tectonics in an extending orogen. *Nature*, *291*(5817), 645.
Wetmore, P. H., Herzig, C., Alsleben, H., Sutherland, M., Schmidt, K. L., Schultz, P. W., & Paterson, S. R. (2003). Mesozoic tectonic evolution of the Peninsular Ranges of southern and Baja California. *Geological Society of America Special Papers*, 93–116.
Wetmore, P. H., Schmidt, K. L., Paterson, S. R., & Herzig, C. (2002). Tectonic implications for the along-strike variation of the Peninsular Ranges batholith, southern and Baja California. *Geology*, *30*(3), 247–250.
Whalen, P. A., & Pessagno, E. A. (1984). Lower Jurassic radiolaria, San Hipolito Formation, Vizcaino Peninsula, Baja California Sur. In V. A. J. Frizzell (Ed.), *Geology of the Baja California peninsula*, *Society of Economic Paleontologists and Mineralogists, Pacific Section* (Vol. 39, pp. 53–66). Los Angeles, CA: Pacific Section, Society of Economic Paleontologists and Mineralogists (SEPM).
Williams, K. M. (1984). Remnants of an apparent eastwest-trending Middle Jurassic subduction and spreading-center system along the west margin of North America: Stanford University Publications. *Geological Sciences*, *18*, 208–211.
Wu, J., Suppe, J., Lu, R., & Kanda, R. (2016). Philippine Sea and East Asian plate tectonics since 52 Ma constrained by new subducted slab reconstruction methods. *Journal of Geophysical Research: Solid Earth*, *121*, 4670–4741. https://doi.org/10.1002/2016JB012923
Zijderveld, J. D. A. (1967). A.C. demagnetization of rocks: Analysis of results. In D. W. Collinson, K. M. Crees, & S. K. Runcorn (Eds.), *Methods in paleomagnetism* (pp. 254–286). Amsterdam: Elsevier.